Learning New Tasks from a Few Examples with Soft-Label Prototypes

Avyav Kumar Singh[1], **Ekaterina Shutova**[2], **Helen Yannakoudakis**[1]
[1]Department of Informatics, King's College London, United Kingdom
[2]ILLC, University of Amsterdam, the Netherlands
avyav_kumar.singh@kcl.ac.uk, e.shutova@uva.nl,
helen.yannakoudakis@kcl.ac.uk

Abstract

Existing approaches to few-shot learning in NLP rely on large language models (LLMs) and/or fine-tuning of these to generalise on out-of-distribution data. In this work, we propose a novel few-shot learning approach based on *soft-label prototypes* (SLPs) designed to collectively capture the distribution of different classes across the input domain space. We focus on learning previously unseen NLP tasks from very few examples (4, 8, 16) per class and experimentally demonstrate that our approach achieves superior performance on the majority of tested tasks in this data-lean setting while being highly parameter efficient. We also show that our few-shot adaptation method can be integrated into more generalised learning settings, primarily meta-learning, to yield superior performance against strong baselines.

1 Introduction

Humans have a remarkable ability to adapt knowledge gained in one domain and apply it in another setting, and to identify or disambiguate objects after observing only a handful of examples (Lake et al., 2015). This has inspired research in few-shot learning that aims to build models that can learn a new task using only a small number of examples per class. Early few-shot learning in NLP relied on interventions at the data level, such as dataset augmentation (Clark et al., 2018) or generation of adversarial examples from few-shot datasets (Miyato et al., 2016), while more recent approaches (van der Heijden et al., 2021; Langedijk et al., 2022) utilise meta-learning (Finn et al., 2017; Snell et al., 2017) to optimise model parameters such that models adapt quickly to new tasks using past experience (Dou et al., 2019; Holla et al., 2020; van der Heijden et al., 2021). The advent of large language models (LLMs) has led to a plethora of further methods, including fine-tuning on different target tasks (Sun et al., 2020; Zhou and Srikumar, 2022), creating prompt-enhanced few-shot datasets for training (Gao et al., 2020; Schick and Schütze, 2020; Lester et al., 2021) as well as parameter-efficient fine-tuning methods for very large language models, with parameters running into billions (Hu et al., 2022; Dettmers et al., 2023).

In this paper, we propose a simple and effective approach to few-shot learning based on *soft-label prototypes* (SLPs) that capture the distribution of different classes across the input domain space, inspired by previous work on generating compact representations of input training data (Sucholutsky et al., 2021). Our contributions are summarised as follows: 1) We develop a novel neural framework for few-shot learning via soft-label prototypes that has a very small computational and memory footprint, and achieves state-of-the-art results in limited-resource settings. Our approach (DeepSLP) does not rely on (expensive) LLM parameter updates or auxiliary training data. 2) We focus on few-shot learning of new, unseen NLP tasks using as little as 4 examples per class, and demonstrate that we outperform strong baselines on the majority of test tasks. 3) We demonstrate that our approach can also be effectively adapted (MetaSLP) in high-resource settings when auxiliary training data is available for few-shot learning, and performs competitively when compared against strong baselines. 4) We release our code and data to facilitate further research in the field.[1]

2 Related work

Early few-shot learning approaches in NLP include data augmentation and semi-supervised learning; e.g., augmentation with adversarial examples (Miyato et al., 2016), interpolation of training data into a learnable higher dimensional embedding space (Chen et al., 2020), and consistency training to

[1] https://github.com/avyavkumar/meta-learned-lines

Proceedings of the 9th Workshop on Representation Learning for NLP (RepL4NLP-2024), pages 215–236
August 15, 2024 ©2024 Association for Computational Linguistics

make models more resistant to noise (Xie et al., 2019). Recent research efforts on large-scale pretraining of language models (Devlin et al., 2019; Radford et al., 2019; Brown et al., 2020; Touvron et al., 2023; BigScience Workshop, 2023; OpenAI, 2024) reduce the amount of data required for their subsequent fine-tuning or utilisation in a given task. Instruction tuning and in-context learning (Brown et al., 2020; Gao et al., 2020; Sanh et al., 2021; Liu et al., 2021; Min et al., 2022; Sun et al., 2024; Zhou et al., 2024) show that natural language instructions or prompts can enhance a model's few-shot learning abilities by leveraging the language (instruction) understanding abilities of the given pretrained LLM (Zhao et al., 2021; Liu et al., 2022). To fine-tune extremely large language models (with billions of parameters) efficiently, a host of parameter-efficient fine-tuning techniques have also been developed (Hu et al., 2022; Dettmers et al., 2023), which leverage pre-trained LLMs and produce superior results on tasks such as question answering, reasoning, text summarisation, coding, etc. (Kotitsas et al., 2024; Jiaramaneepinit et al., 2024; Yang et al., 2024; Ding et al., 2023).

However, the search space over LLMs, prompt templates and few-shot learning is so great that there is yet to be an established standard. Different models require different styles of (few-shot) prompting, and certain prompt templates may work better with specific LLMs and datasets rather than universally across the board (e.g., Davis et al. (2024)). Furthermore, evaluating robustness of state-of-the-art / generative LLMs on new, unseen tasks (OOD generalisation) presents a significant challenge due to their vast and unknown training data, resulting in artificially inflated performance as a result of data leakage (Yang et al., 2023).

Previous work has also tackled few-shot learning within the meta-learning paradigm of *"learning to learn"* (Schmidhuber, 1987; Bengio et al., 1990; Thrun and Pratt, 1998), utilising methods that are trained to adapt quickly (in a few gradient steps) to new tasks and from a small number of examples, using past experience. Meta-learning has emerged as a promising technique for a range of tasks (Finn et al., 2017; Koch et al., 2015; Ravi and Larochelle, 2017), including NLP such as natural language inference, text classification, etc. (Obamuyide and Vlachos, 2019a,b; Holla et al., 2020; Bansal et al., 2020b; Nooralahzadeh et al., 2020; Wang et al., 2020; Langedijk et al., 2022; Mueller et al., 2023).

In a similar spirit to parameter-efficient fine-tuning (Hu et al., 2022; Dettmers et al., 2023), our work shifts away from the aforementioned paradigms that suffer from lack of standardisation (LLM few-shot prompting) and increased computational complexity for fine-tuning (e.g., fine-tuning extremely large language models such as GPT (OpenAI, 2024). We present a novel, parameter-efficient few-shot learning framework (DeepSLP) based on soft-label prototypes (SLPs), which we show to be effective on a range of tasks in limited and high-resource settings, while having a substantially smaller computational and memory footprint. While DeepSLP does not rely on LLM fine-tuning or auxiliary training data, we present a variant (MetaSLP) that can be used for few-shot learning via auxiliary data and fine-tuned encoders.

We target few-shot learning of new, unseen tasks (i.e., tasks and classes not previously trained on) (a) in limited-resource settings, without access to auxiliary training data, and with frozen model parameters, and (b) in high-resource settings, with access to auxiliary training data, which are used to update model parameters. For the latter, our work is similar to Bansal et al. (2020a). The authors target few-shot learning of unseen tasks via meta-learning, utilising auxiliary training data.

3 Approach: few-shot learning with Soft-Label Prototypes (SLPs)

A soft label is defined as a vector Y representing a data point's simultaneous membership to several classes (Sucholutsky and Schonlau, 2021), essentially denoting a point's partial association to different classes. Using this definition, a soft-label prototype (SLP) is defined as $(\vec{X}, Y)$, where $\vec{X}$ is a point in input space (e.g., an input feature vector) and Y is its corresponding soft label. The underlying idea in Sucholutsky and Schonlau (2021)'s work is that a small set of soft-label prototypes can be used to accurately represent a training set. We build on this idea and reframe SLPs for the task of few-shot learning of new, unseen tasks where very small amounts of data are available per class.

3.1 Generating soft-label prototypes

Soft-label prototypes assign soft labels to every point in the input domain; therefore, a soft-label prototype at point $\vec{X}$ represents the class distribution (determined from the training data) at $\vec{X}$. The fundamental idea behind a "soft-label" is that, unlike hard labels, which are one-hot encoded la-

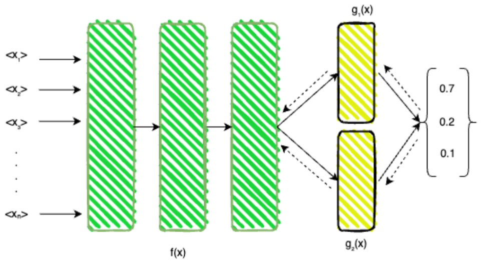

Figure 1: Learning soft-label prototypes using two trainable linear layers (yellow): example for a 3-class prototype. Dotted lines indicate backpropagation.

bels, soft-labels contain a distribution of probabilistic label values at a particular point in a high-dimensional embedding space.

The process of generating soft-label prototypes from training data can be split into a two step process (Sucholutsky et al., 2021): (1) finding lines that connect the class centroids in the training data, where each line connects some of the centroids, and every centroid belongs to one line; and (2) using linear constraints to derive soft-label prototypes capturing the class distribution at the ends of each line. The two steps are presented in detail below.

3.1.1 Finding lines connecting all centroids

Here we seek to find classes that lie on the same manifold. First, we compute the centroid of each class in the input training data. Then, we find and fit class centroids on the minimum number of lines using recursive regression (Sucholutsky et al., 2021). This method clusters centroids hierarchically to group similar (interval) centroids together, and fits a regression line on the centroids. The similarity of centroids within a single cluster is judged by how well all the centroids fit on a regression line. If the Euclidean distance of a particular centroid is beyond a pre-defined tolerance threshold ϵ from a line, it is removed from that cluster and assigned to another one. We use this method for all our experiments, as we experimentally find (on our dev data) that it performs well on high-dimensional data spread across many classes such as the ones we test here. In Appendix A.1, Figure 3a, we present an example set of lines connecting all centroids.

3.1.2 Learning soft-label prototypes

Once we find the lines, we use the endpoints of each line as the location of soft-label prototypes. Therefore, for l lines fitted on n centroids we have $2l$ prototypes. Then, we need to find the class distribution at each end point / soft-label prototype. We develop and experiment with two different approaches to finding the class distributions, one based on constraint optimisation (*constraintSLP*), and another based on gradient descent (*DeepSLP*).

Learning via linear constraints (constraintSLP) One way in which we can approach this is via constraint optimisation and, specifically, an optimisation problem that consists of two main sets of constraints (Sucholutsky et al., 2021): (i) the target class at each centroid has the maximum influence amongst all classes at certain points along the line (endpoint of the line and midpoints between classes); and (ii) the difference between the influence of the target class and the sum of the influences of all other classes along the line is maximised. In order to make this approach powerful enough for large, high-dimensional NLP data, we require an optimiser that scales on such complex data. To this end, we use the MOSEK solver for linear programming (MOSEK ApS, 2019) in the CVXPY library (Diamond and Boyd, 2016) to perform the required computations to generate the soft-label prototype class distributions. The output of this is then a set of soft-label prototypes which "sit" at the ends of each line (i.e., $\vec{X}$) as shown in Appendix A.1, Figure 3b.

Learning via gradient descent (DeepSLP) Rather than use linear constraints to generate soft-label prototypes, we develop a novel gradient-based approach to generate soft labels as a function of an input x by minimising training loss on a few-shot dataset. After generating lines connecting all class centroids (Section 3.1.1), we set two soft-label prototypes at the ends of the lines. Each soft-label prototype p_i is denoted by $g_i(f(x))$ where g is a neural network parameterised by θ_i and $f(x)$ is a point in the input space. The neural network consists of a fixed BERT (Devlin et al., 2019) encoder[2] given by $f(x)$, and a trainable linear layer which returns the soft-label probability distribution at any point x given by $g_i(x)$. Figure 1 presents a visual representation of our model. Compared to constraintSLP where we find soft-label probability distributions via linear constraint optimisation, we now parameterise our soft-label probability distribution with a neural network.

[2] We use BERT as our encoder given its comparatively higher computational efficiency, and do not include LLMs such as Llama and the GPT family as they have already been pre-trained on our test tasks (found here) and hence suffer from data contamination.

Algorithm 1: DeepSLP

```
$\lambda \leftarrow$ set of lines connecting all centroids
$f_{\theta_l}$ is the network parameterised by $\theta_l$ for
    the left-end prototype on a line
$f_{\theta_r}$ is the network parameterised by $\theta_r$ for
    the right-end prototype on a line
$\mathcal{J} \leftarrow$ loss function
$D \leftarrow$ training data
Require $\lambda \neq \emptyset$
for $i \in \lambda$ do
    for $epoch$ $1.....N$ do
        $p_{il} \leftarrow$ location of left prototype
        $p_{ir} \leftarrow$ location of right prototype
        for $x \in minibatch(D)$ do
            $d_1 \leftarrow ||p_{il} - x||$
            $d_2 \leftarrow ||p_{ir} - x||$
            $pred.append\left(\frac{f_{\theta_{il}}(x)}{d_1} + \frac{f_{\theta_{ir}}(x)}{d_2}\right)$
        end
        $d\_loss \leftarrow \mathcal{J}(pred, D)$
        $loss_1 \leftarrow \frac{d_2}{d_1+d_2} * d\_loss$
        $loss_2 \leftarrow \frac{d_1}{d_1+d_2} * d\_loss$
        $\theta_{il} \leftarrow \theta_{il} - \eta\nabla_{\theta_{il}} loss_1$
        $\theta_{ir} \leftarrow \theta_{ir} - \eta\nabla_{\theta_{ir}} loss_2$
    end
end
```

Crucially, the encoder parameters are frozen as we need our input data points to have an unchanged location in the input space – changing their position might result in class centroids that were previously lying on a straight line to no longer lie on the line. The model is optimised using both soft-label prototypes along a line (see Algorithm 1 below and Section 3.2, Equation 1). Specifically, a higher distance between a data point x and a prototype leads to a correspondingly smaller effect of the prototype on the final classification; therefore, we want to penalise the prototype that is closer to x more if there is an incorrect classification. Each prototype is therefore assigned a fraction of the total loss that is proportional to the other prototype's Euclidean distance from x. This way, the closer prototype's weights are corrected more in case of a misclassification. The complete algorithm can be seen in Algorithm 1, while an example optimisation is presented in Figure 2.

We use cross entropy loss which gives a measure of the difference between the true and predicted labels. We initialise the weights of $g_1(x)$ and $g_2(x)$ using a uniform Xavier initialisation (Glorot and Bengio, 2010) and use warmup steps to adjust the learning rate. Epochs vary based on the number of classes in the classifier head (between 15 and 25; see datasets used in Section 4): preliminary experiments on the development data show that more epochs are needed when a higher number of classes lie along a line.

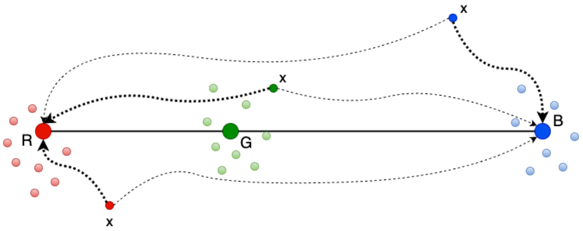

Figure 2: Training soft-label prototypes in DeepSLP. Class centroids are represented with large circles that lie on a line (**R**ed, **G**reen, **B**lue), while training set examples are represented with smaller circles of the same colour. Dotted lines represent the backpropagation error, of which the bolded ones represent a larger error per soft-label prototype. Predictions for x are based on the prototypes at each end of the line.

3.2 Classification with soft-label prototypes

Given M soft-label prototypes representing the input distribution of N classes, we define $S = (\vec{X}_1, Y_1), ..., (\vec{X}_M, Y_M)$ to be our set of prototypes, where $\vec{X}_i$ is the location of the i^{th} prototype in the input feature space and Y_i is a matrix of dimension $[N \times 1]$ denoting the soft labels. Given a test datapoint $\vec{x}$, we calculate the Euclidean distances $D = (\vec{X}_i, \vec{x})_{i=1,2...M}$ from each prototype to $\vec{x}$. We then sort S in ascending order of distances using D, weigh the probability distribution of the i^{th} nearest prototype inversely by its distance to $\vec{x}$, and select the line containing the closest prototype to get Y^* (Sucholutsky et al., 2021):

$$Y^* = \sum_{i=1}^{k} \frac{Y_i}{d(\vec{X}_i, \vec{x})} \quad (1)$$

As we consider the two nearest neighbours / prototypes, we set k to 2. $\vec{x}$ is then assigned the class $C^{SLP}(\vec{x}) = \underset{j}{\text{argmax}} Y_j^*$ where Y_j^* is the j$^{\text{th}}$ element of Y^*. In other words, we sum over the k-nearest soft-label prototypes (i.e., vectors) to $\vec{x}$, and weigh each prototype inversely proportional to its distance from $\vec{x}$. $\vec{x}$ is then assigned the class with the largest value in the resulting vector (see Appendix A.1 for a toy classification example).

3.3 Meta-training DeepSLP (MetaSLP)

We further test the suitability of soft-labels in high-resource settings, tuning our text encoder using auxiliary training data. This is similar to the work of (Bansal et al., 2020a) that develop a meta-learning approach for few-shot learning of new, unseen tasks while utilising auxiliary training data. We employ a similar approach for rapid generalisation by utilising first-order meta-learning algorithms (which we describe in detail in Appendix A.2). Our model architecture is similar to DeepSLP – it comprises a BERT encoder with two linear layers on top. We train only the last v layers of our encoder to reduce computational overhead, where v is a hyperparameter (See Appendix A.6). We denote the encoder by $f_\theta(x)$, and each soft-label prototype at the end of a line by g_1 and g_2, parameterised by θ_1 and θ_2 respectively. The difference between DeepSLP and MetaSLP is that MetaSLP is trained using meta-learning (using auxiliary data described in Section 4), and the encoder $f_\theta(x)$ in MetaSLP is fine-tuned (as opposed to being fixed in DeepSLP), following previous work (Bansal et al., 2020a).

Inner-loop training We optimise the soft-label prototypes in the same manner as DeepSLP; i.e., we use Algorithmn 1 to few-shot train the linear layers $g_1(x)$ and $g_2(x)$ parameterised by θ_1 and θ_2 respectively. However, meta-learning requires a large set of diverse and balanced meta-learning tasks for effective learning (Holla et al., 2020). To ameliorate this, we split the auxiliary datasets (Section 4) used for meta-learning into multiple pairwise tasks to meta-train MetaSLP (Bansal et al., 2020a). This means that, during training, we now consider a large number of two-class problems, as opposed to a small number of multi-class problems where the number of classes $n \geq 2$. Such a setting also enables fine-tuning of our encoder $f_\theta(x)$. In general, allowing the physical location of encodings to change (in this case via meta-learning's inner-loop training process), may result in centroids originally connected by a line to no longer be connected by that line (i.e., in the next inner-loop optimisation step). However, if we only meta-train on tasks that focus on two classes at a time, this can trivially ensure that the same line is utilised each time. Our inner-loop optimisation process is given in Algorithm 3 in Appendix A.4.

Outer-loop training We perform meta-learning using the updated parameters in the inner-loop training process. We experiment with both Reptile (Nichol et al., 2018) and FOMAML (Finn et al., 2017) as our meta-learning algorithms. Reptile can be considered a simpler variant to MAML-based meta-learning algorithms. We present our outer-loop process in Algorithm 4, Appendix A.4.

Meta-testing We construct lines for the test sets using the trained MetaSLP model, and fine-tune them on the few-shot adaptation training data for each test task. We then use these lines for classification as described in Section 3.2.

4 Experimental settings and datasets

Experimental settings We experiment with two settings in terms of amounts of available data. The first is a limited-resource setting where we only train / fine-tune our models in a few-shot manner on small amounts of training data (i.e., in the absence of auxiliary training data). The other setting is a high-resource setting where we assume that auxiliary training data is available for additional training / fine-tuning.

Datasets We tackle few-shot learning of previously unseen tasks (i.e., not seen during training/fine-tuning), and so our work is similar to Bansal et al. (2020a). For our high-resource setting, we train and test our models on the same data as Bansal et al. (2020a) to ensure direct comparability. For our limited-resource setting, we test in the same way but do not utilise any auxiliary training data; i.e., we only utilise few-shot fine-tuning data for unseen tasks (i.e., only using a very small set of training/fine-tuning examples for the test tasks).

High-resource setting auxiliary training data Similar to Bansal et al. (2020a), we use GLUE (Wang et al., 2018) to train our models in the high-resource setting. This dataset consists of a range of natural language tasks such as entailment, classification and textual similarity, which are used for model training and evaluation. We use only the training split for meta-learning. Similar to Bansal et al. (2020a), the MNLI (Williams et al., 2018) and SNLI (Bowman et al., 2015) entailment tasks, which are three-label classification problems, are split in a pairwise manner such that they are included as multiple two-label datasets during training. Following Bansal et al. (2020a), we also train for detecting the sentiment contained within phrases of a sentence by using the phrase-level annotations in SST2 (Wang et al., 2018). We utilise the same validation sets – labelled Amazon review data from music, toys and videos for sentiment classification (Blitzer et al., 2007). We provide dataset and training details in Appendix A.5.

Evaluation data We use the same test datasets and evaluation setting as Bansal et al. (2020a) for both the high-resource and low-resource settings. These cover a variety of text classification tasks: (a) *Entity typing* – the CoNLL-2003 (Tjong Kim Sang and De Meulder, 2003) and MIT-Restaurant (Liu et al., 2013) datasets; (b) *Review rating classification* – review ratings from Amazon Reviews (Blitzer et al., 2007) with a three-way classification; (c) *Text classification* – scraped social media data from crowdflower comprising sentiment and emotion classification in a range of domains, as well as political bias detection; and (d) *Natural language inference* in the scientific domain – the SciTail dataset (Khot et al., 2018). We use the same data splits, which are publicly available. During evaluation, Bansal et al. (2020a) fine-tune their models using a small few-shot (support) training set per test task (using a k-shot setting of $4, 8, 16$ examples per class), and then evaluate performance on each task's dedicated, unseen test set. As model performance can be affected by the k examples chosen for training/fine-tuning, for each task and for every k, they sample 10 few-shot training sets and report the mean and standard deviation, which we also adopt in our experiments.

5 Baselines

Our aim is to determine how well our models – DeepSLP and MetaSLP – perform in the low and high-resource setting respectively, compared to strong baselines when given the same few-shot adaptation sets. Our focus is on (a) evaluating in an extreme few-shot learning scenario where no auxiliary data is available (using DeepSLP), and (b) evaluating in a high-resource setting when additional (auxiliary) training data is available (MetaSLP). We use BERT (Devlin et al., 2019) as our text encoder throughout to facilitate model comparisons. We report DeepSLP and MetaSLP$_{\text{REPTILE}}$ (i.e., using Reptile as our meta-learning algorithm) in our main table of results (given their effectiveness), and present additional baselines as well as hyperparameters and training details in Appendix A.6.

We use BERT (Devlin et al., 2019) as our encoder as it is a text encoder that allows us to get passage-level encodings, it is computationally lightweight compared to decoder-based LLMs such as Llama (Touvron et al., 2023) and GPT (OpenAI, 2024) (and we can carry out full fine-tuning) and, crucially, it does not suffer from data contamination as, in contrast to the more recent LLMs, it has not been pre-trained on our test data[3].

5.1 Low-resource setting baselines

BERT$_{\text{fine-tuned}}$ We use BERT$_{\text{fine-tuned}}$ reported in Bansal et al. (2020a), which is fine-tuned (all layers) on the few-shot training set of each test task.

LORA$_{\text{BERT}}$ LORA (Hu et al., 2022) decomposes a fine-tuned weight matrix to two low-rank matrices, which – when multiplied and added to the original weights – reproduce the fine-tuned weights. This is advantageous as, instead of fine-tuning all parameters, we fine-tune these two matrices with a low computational cost, as they are much smaller individually compared to fully fine-tuned weights.

constraintSLP We use constraintSLP as a baseline to evaluate the effectiveness of soft-label prototypes that are based on linear constraints.

5.2 High-resource setting baselines

Reptile We train a meta-learning Reptile (Nichol et al., 2018) model on our auxiliary data and use it as another baseline. This allows us to directly assess the added advantage of utilising SLPs in MetaSLP$_{\text{REPTILE}}$.

Prototypical Networks We use ProtoNet (Snell et al., 2017) as another baseline *for both* the high and low-resource settings. ProtoNets use Euclidean distance as a measure of similarity between points and clusters, which is similar to DeepSLP and MetaSLP that assign test points to the closest line.

LEOPARD Bansal et al. (2020a) present LEOPARD, a meta-learning algorithm that achieves the best performance across most test tasks for entity typing, ratings classification and text classification, and which we also use.

We do not include HSMLMT (Bansal et al., 2020b) as a baseline as it is pretrained on semi-supervised meta-training tasks in addition to supervised learning and therefore it is not directly comparable.

[3] https://github.com/iesl/leopard/tree/master/data/json

Category (Classes)	**Shot**	**LORA$_{\text{BERT}}$**	**BERT$_{\text{fine-tuned}}$***	**DeepSLP**	**LEOPARD***	**Reptile**	**MetaSLP$_{\text{REPTILE}}$**
Political Bias (2)	4	52.75 ± 4.33	54.57 ± 5.02	53.251 ± 4.042	60.49 ± 6.66	58.82 ± 4.31	60.96 ± 6.13
	8	53.66 ± 4.25	56.15 ± 3.75	58.209 ± 5.198	61.74 ± 6.73	59.43 ± 3.79	63.65 ± 4.57
	16	59.21 ± 2.27	60.96 ± 4.25	61.479 ± 2.974	65.08 ± 2.14	62.21 ± 0.72	66.05 ± 1.57
Emotion (13)	4	7.56 ± 2.93	09.20 ± 3.22	9.076 ± 1.108	11.71 ± 2.16	11.65 ± 3.21	11.94 ± 1.95
	8	9.02 ± 2.36	08.21 ± 2.12	8.041 ± 2.797	12.90 ± 1.63	10.56 ± 2.85	13.42 ± 1.46
	16	10.29 ± 1.67	13.43 ± 2.51	10.919 ± 1.615	13.38 ± 2.20	11.62 ± 3.11	14.03 ± 2.35
Sentiment Books (2)	4	51.27 ± 2.75	54.81 ± 3.75	58.67 ± 4.753	82.54 ± 1.33	76.95 ± 1.03	83.22 ± 0.95
	8	58.16 ± 3.3	53.54 ± 5.17	64.78 ± 2.615	83.03 ± 1.28	77.49 ± 1.08	83.8 ± 0.8
	16	59.16 ± 2.59	65.56 ± 4.12	67.453 ± 3.085	83.33 ± 0.79	77.88 ± 0.56	83.8 ± 1.59
Rating DVD (3)	4	31.65 ± 4.91	32.22 ± 08.72	39.566 ± 5.086	49.76 ± 9.80	45.91 ± 9.85	45.2 ± 8.91
	8	37.69 ± 3.16	36.35 ± 12.50	38.788 ± 4.449	53.28 ± 4.66	47.23 ± 9.22	58.38 ± 2.9
	16	38.63 ± 5.52	42.79 ± 10.18	40.53 ± 4.375	53.52 ± 4.77	48.49 ± 8.88	57.41 ± 4.71
Rating Electronics (3)	4	31.66 ± 2.94	39.27 ± 10.15	39.977 ± 5.959	51.71 ± 7.20	44.47 ± 8.25	45.34 ± 7.22
	8	38.72 ± 5.95	28.74 ± 08.22	41.926 ± 3.985	54.78 ± 6.48	49.1 ± 6.81	55.10 ± 5.12
	16	39.15 ± 6.6	45.48 ± 06.13	44.917 ± 3.164	58.69 ± 2.41	50.68 ± 6.8	59.47 ± 2.29
Rating Kitchen (3)	4	36.63 ± 4.68	34.76 ± 11.20	39.624 ± 6.787	50.21 ± 09.63	45.38 ± 10.96	45.20 ± 8.78
	8	39.69 ± 6.22	34.49 ± 08.72	41.081 ± 6.777	53.72 ± 10.31	46.71 ± 9.84	54.53 ± 9.9
	16	38.17 ± 7.14	47.94 ± 08.28	45.801 ± 4.562	57.00 ± 08.69	52.87 ± 9.52	58.94 ± 7.58
Political Audience (2)	4	49.75 ± 1.03	51.02 ± 1.72	51.741 ± 2.827	52.60 ± 3.51	52.45 ± 4.26	54.1 ± 3.66
	8	54.05 ± 2.54	52.80 ± 2.72	54.506 ± 3.274	54.31 ± 3.95	52.87 ± 4.31	56.01 ± 3.65
	16	55.39 ± 3.66	58.45 ± 4.98	56.956 ± 3.045	57.71 ± 3.52	55.6 ± 1.85	58.57 ± 2.04
Sentiment Kitchen (2)	4	53.02 ± 1.54	56.93 ± 7.10	60.76 ± 4.426	78.35 ± 18.36	69.81 ± 14.58	81.96 ± 3.73
	8	55.54 ± 3.47	57.13 ± 6.60	65.733 ± 3.198	84.88 ± 1.12	75.76 ± 1.13	83.33 ± 1.99
	16	58.59 ± 4.83	68.88 ± 3.39	69.18 ± 2.589	85.27 ± 1.31	76.41 ± 0.66	84.33 ± 1.81
Disaster (2)	4	56.02 ± 6.35	55.73 ± 10.29	54.252 ± 9.843	51.45 ± 4.25	49.76 ± 4.73	55.03 ± 8.73
	8	57.46 ± 6.9	56.31 ± 09.57	61.3 ± 7.961	55.96 ± 3.58	52.17 ± 5.17	57.77 ± 6.40
	16	65.79 ± 2.03	64.52 ± 08.93	69.28 ± 2.358	61.32 ± 2.83	55.37 ± 4.53	65.18 ± 4.41
Airline (3)	4	24.36 ± 5.42	42.76 ± 13.50	50.987 ± 4.936	54.95 ± 11.81	57.11 ± 14.16	57.39 ± 7.83
	8	52.31 ± 7.89	38.00 ± 17.06	55.209 ± 6.049	61.44 ± 03.90	64.37 ± 3.49	65.67 ± 4.82
	16	54.1 ± 8.57	58.01 ± 08.23	60.247 ± 4.577	62.15 ± 05.56	66.31 ± 2.55	69.48 ± 2.06
Rating Books (3)	4	34.69 ± 2.12	39.42 ± 07.22	42.116 ± 4.725	54.92 ± 6.18	56.57 ± 8.17	55.79 ± 5.61
	8	39.36 ± 6.33	39.55 ± 10.01	42.156 ± 4.608	59.16 ± 4.13	57.33 ± 7.63	65.74 ± 5.58
	16	41.23 ± 5.32	43.08 ± 11.78	46.513 ± 3.036	61.02 ± 4.19	63.26 ± 3.59	67.87 ± 3.45
Political Message (9)	4	12.16 ± 1.46	15.64 ± 2.73	14.421 ± 1.095	15.69 ± 1.57	14.58 ± 1.78	18.84 ± 1.82
	8	15.71 ± 2.04	13.38 ± 1.74	16.919 ± 1.756	18.02 ± 2.32	15.13 ± 2.16	20.09 ± 2.71
	16	15.53 ± 2.55	20.67 ± 3.89	18.319 ± 1.74	18.07 ± 2.41	16.38 ± 2.15	23.22 ± 1.17
Sentiment DVD (2)	4	50.77 ± 0.78	54.98 ± 3.96	55.003 ± 2.936	80.32 ± 1.02	72.03 ± 11.61	80.97 ± 1.21
	8	52.24 ± 1.54	55.63 ± 4.34	57.527 ± 3.562	80.85 ± 1.23	75.79 ± 1.62	81.85 ± 1.79
	16	52.6 ± 2.09	58.69 ± 6.08	60.76 ± 2.944	81.25 ± 1.41	76.69 ± 0.8	83.48 ± 1.01
Scitail (2)	4	43.36 ± 4.74	58.53 ± 09.74	54.101 ± 3.759	69.50 ± 9.56	59.13 ± 10.58	53.48 ± 5.59
	8	54.29 ± 5.25	57.93 ± 10.70	56.341 ± 5.786	75.00 ± 2.42	62.63 ± 10.85	60.79 ± 4.6
	16	52.68 ± 3.0	65.66 ± 06.82	59.692 ± 4.227	77.03 ± 1.82	68.03 ± 1.57	61.67 ± 3.61
Restaurant (8)	4	10.56 ± 1.36	49.37 ± 4.28	47.634 ± 5.237	49.84 ± 3.31	13.37 ± 2.25	27.00 ± 2.61
	8	20.92 ± 2.4	49.38 ± 7.76	55.912 ± 4.494	62.99 ± 3.28	16.83 ± 3.42	35.66 ± 2.39
	16	29.37 ± 4.05	69.24 ± 3.68	61.716 ± 2.208	70.44 ± 2.89	16.0 ± 3.44	37.20 ± 2.68
CoNLL (4)	4	21.48 ± 2.71	50.44 ± 08.57	52.724 ± 5.84	54.16 ± 6.32	31.31 ± 5.32	40.79 ± 3.40
	8	29.84 ± 3.28	50.06 ± 11.30	60.374 ± 3.731	67.38 ± 4.33	33.17 ± 5.1	41.25 ± 5.21
	16	37.18 ± 3.32	74.47 ± 03.10	67.496 ± 4.551	76.37 ± 3.08	34.04 ± 3.59	45.96 ± 4.75

Table 1: Classification performance (accuracy) of our methods (DeepSLP and MetaSLP) and baselines. * refers to the baselines as reported in Bansal et al. (2020a). The best performing models for each setting (without and with auxiliary data) are highlighted in gray and green respectively. Double lines group similar tasks together: the first set contains intent classification tasks, the second focuses on natural language inference, and the last contains entity typing tasks.

6 Results and Discussion

Due to space restrictions, we present and discuss our best models in Table 1. All other baselines and results are discussed in Appendix A.7.

Low-resource setting In the low-resource setting with no auxiliary data (left side of Table 1), DeepSLP outperforms all baselines, including $\text{BERT}_{\text{fine-tuned}}$ in $31/48$ tasks and $\text{LORA}_{\text{BERT}}$ in $45/48$ tasks, achieving a new state-of-the-art result. Our results demonstrate the usefulness of soft-label prototypes and their superiority over strong baselines (i.e., LLM fine-tuning and LORA / low-rank adaptation) in the low-resource setting.

Unlike $\text{BERT}_{\text{fine-tuned}}$, DeepSLP and $\text{LORA}_{\text{BERT}}$ do not fine-tune the encoder. Specifically, we only need to fine-tune $1500-10K$ parameters (based on the number of classes) for each line with two soft-label prototypes for DeepSLP, compared to $50K-100K$ parameters for $\text{LORA}_{\text{BERT}}$ with $rank = 2$, and $> 10^8$ parameters for $\text{BERT}_{\text{fine-tuned}}$. We also note that DeepSLP is lightweight and does not require a GPU. $\text{LORA}_{\text{BERT}}$ mostly achieves accuracies within 90% of $\text{BERT}_{\text{fine-tuned}}$, in line with previous work (Hu et al., 2022; Dettmers et al., 2023) (even outperforming $\text{BERT}_{\text{fine-tuned}}$ in $15/48$ tasks), except for entity-typing tasks where $\text{LORA}_{\text{BERT}}$ struggles to generalise and achieves substantially lower performance compared to $\text{BERT}_{\text{fine-tuned}}$.

On the other hand, constraintSLP, a simpler variant of DeepSLP (see Appendix A.7, Table 5 for results) is one of the lower performing baselines, together with ProtoNet. We find that constraintSLP exhibits a substantial weakness (see further details in Theorem A.2, Appendix A.3): given Euclidean distance, constraintSLP does not always select the nearest class centroid to a test point. This violates our inductive bias that points located closest to a class centroid are assigned to that class. If we consider the case where $N = 2$, constraintSLP essentially acts as a 1-NN with soft labels trivially at $[1, 0]$ and $[0, 1]$, with class centroids acting as the nearest neighbour. However, when generalising beyond this setting, the model's stability is affected. constraintSLP optimises soft labels using the geometric properties of a line and does not consider each (training) data point individually – the soft labels produced by SLP are constants. DeepSLP, on the other hand, learns from training data and produces soft labels as a function of the input; therefore, it has the ability to output soft labels based on the location of an input (test) point (with the location of the prototypes being fixed).

High-resource setting $\text{MetaSLP}_{\text{REPTILE}}$ has the highest performance overall in text classification and entailment tasks (Tasks 1-14), with the best accuracy in $33/42$ tasks/settings. LEOPARD, on the other hand, achieves the highest score in only $8/42$. Interestingly, we find that all models in the high-resource setting have lower performance for *Disaster* compared to the models in the low-resource setting. We surmise this to be due to the auxiliary data and the fact that the meta-training distribution differs substantially from the test distribution.

For entity typing tasks (CoNLL and Restaurant), LEOPARD outperforms all models, with $\text{MetaSLP}_{\text{REPTILE}}$ and Reptile performing comparatively poorly, even outperformed by the low-resource methods (DeepSLP and $\text{BERT}_{\text{fine-tuned}}$). It should be noted that there seems to be little benefit of meta-learning with auxiliary data when tackling entity typing tasks, even for LEOPARD, as the difference between LEOPARD and $\text{BERT}_{\text{fine-tuned}}$ is not substantial. We surmise this to be due to the fact that the meta-training distribution (i.e., GLUE tasks) is different from the test distribution for entity typing tasks which degrades performance for the test tasks. Note that we do not meta-train the entire model (only top 4 layers for Reptile and $\text{MetaSLP}_{\text{REPTILE}}$), unlike LEOPARD.

Overall, $\text{MetaSLP}_{\text{REPTILE}}$ outperforms all models and baselines, including Reptile in $42/48$ tasks and LEOPARD in $34/48$ tasks. Specifically, $\text{MetaSLP}_{\text{REPTILE}}$ consistently outperforms Reptile, demonstrating the effectiveness of our approach over its meta-learning variant (i.e., Reptile) that does not use SLPs. In Appendix A.8 we present detailed analyses of DeepSLP and show that it displays several desirable properties of ensemble methods which drive its performance, in addition to it being a computationally efficient approach that only utilises a small number of parameters.

7 Conclusion and future work

We presented a novel few-shot learning paradigm that is based on soft-label prototypes capturing the simultaneous membership of data points over several classes, and demonstrated its effectiveness in low and high-resource settings. We evaluated our approach on 48 different tasks / settings and showed that it outperforms a range of strong baselines. In the future, we plan to use meta-learning algorithms such as PACMAML (Ding et al., 2021) and Bayesian MAML (Kim et al., 2018) that relax assumptions with respect to train–test set distributions and thus alleviate this current limitation in our work.

8 Ethics

To the best of our knowledge, there are no ethical concerns involved in this research. We conduct our work using publicly available English datasets and tasks, and models pre-trained on English text. Our results may not generalise to other languages. To facilitate further research in the field, we release our source code and models.

References

Taiga Abe, Estefany Kelly Buchanan, Geoff Pleiss, Richard Zemel, and John P Cunningham. 2022. Deep ensembles work, but are they necessary? In *Advances in Neural Information Processing Systems*, volume 35, pages 33646–33660. Curran Associates, Inc.

Antreas Antoniou, Harrison Edwards, and Amos Storkey. 2019. How to train your MAML. In *International Conference on Learning Representations*.

Arsenii Ashukha, Alexander Lyzhov, Dmitry Molchanov, and Dmitry Vetrov. 2020. Pitfalls of in-domain uncertainty estimation and ensembling in deep learning. *arXiv preprint arXiv:2002.06470*.

Trapit Bansal, Rishikesh Jha, and Andrew McCallum. 2020a. Learning to few-shot learn across diverse natural language classification tasks. In *Proceedings of the 28th International Conference on Computational Linguistics*, pages 5108–5123, Barcelona, Spain (Online). International Committee on Computational Linguistics.

Trapit Bansal, Rishikesh Jha, Tsendsuren Munkhdalai, and Andrew McCallum. 2020b. Self-supervised meta-learning for few-shot natural language classification tasks.

Yoshua Bengio, Samy Bengio, and Jocelyn Cloutier. 1990. *Learning a synaptic learning rule*. Citeseer.

BigScience Workshop. 2023. Bloom: A 176b-parameter open-access multilingual language model.

John Blitzer, Mark Dredze, and Fernando Pereira. 2007. Biographies, Bollywood, boom-boxes and blenders: Domain adaptation for sentiment classification. In *Proceedings of the 45th Annual Meeting of the Association of Computational Linguistics*, pages 440–447, Prague, Czech Republic. Association for Computational Linguistics.

Samuel R. Bowman, Gabor Angeli, Christopher Potts, and Christopher D. Manning. 2015. A large annotated corpus for learning natural language inference.

Tom B. Brown, Benjamin Mann, Nick Ryder, Melanie Subbiah, Jared Kaplan, Prafulla Dhariwal, Arvind Neelakantan, Pranav Shyam, Girish Sastry, Amanda Askell, Sandhini Agarwal, Ariel Herbert-Voss, Gretchen Krueger, Tom Henighan, Rewon Child, Aditya Ramesh, Daniel M. Ziegler, Jeffrey Wu, Clemens Winter, Christopher Hesse, Mark Chen, Eric Sigler, Mateusz Litwin, Scott Gray, Benjamin Chess, Jack Clark, Christopher Berner, Sam McCandlish, Alec Radford, Ilya Sutskever, and Dario Amodei. 2020. Language models are few-shot learners.

Jiaao Chen, Zichao Yang, and Diyi Yang. 2020. Mixtext: Linguistically-informed interpolation of hidden space for semi-supervised text classification.

Kevin Clark, Minh-Thang Luong, Christopher D. Manning, and Quoc V. Le. 2018. Semi-supervised sequence modeling with cross-view training.

Christopher Davis, Andrew Caines, Øistein Andersen, Shiva Taslimipoor, Helen Yannakoudakis, Zheng Yuan, Christopher Bryant, Marek Rei, and Paula Buttery. 2024. Prompting open-source and commercial language models for grammatical error correction of english learner text.

Tim Dettmers, Artidoro Pagnoni, Ari Holtzman, and Luke Zettlemoyer. 2023. Qlora: Efficient finetuning of quantized llms. In *Advances in Neural Information Processing Systems*, volume 36, pages 10088–10115. Curran Associates, Inc.

Jacob Devlin, Ming-Wei Chang, Kenton Lee, and Kristina Toutanova. 2019. BERT: Pre-training of deep bidirectional transformers for language understanding. In *Proceedings of the 2019 Conference of the North American Chapter of the Association for Computational Linguistics: Human Language Technologies, Volume 1 (Long and Short Papers)*, pages 4171–4186, Minneapolis, Minnesota. Association for Computational Linguistics.

Steven Diamond and Stephen Boyd. 2016. CVXPY: A Python-embedded modeling language for convex optimization. *Journal of Machine Learning Research*, 17(83):1–5.

Thomas G. Dietterich. 2000. Ensemble methods in machine learning. In *Multiple Classifier Systems*, pages 1–15, Berlin, Heidelberg. Springer Berlin Heidelberg.

Nan Ding, Xi Chen, Tomer Levinboim, Sebastian Goodman, and Radu Soricut. 2021. Bridging the gap between practice and pac-bayes theory in few-shot meta-learning. In *Advances in Neural Information Processing Systems*, volume 34, pages 29506–29516. Curran Associates, Inc.

Ning Ding, Xingtai Lv, Qiaosen Wang, Yulin Chen, Bowen Zhou, Zhiyuan Liu, and Maosong Sun. 2023. Sparse low-rank adaptation of pre-trained language models. In *Proceedings of the 2023 Conference on Empirical Methods in Natural Language Processing*, pages 4133–4145, Singapore. Association for Computational Linguistics.

William B. Dolan and Chris Brockett. 2005. Automatically constructing a corpus of sentential paraphrases. In *Proceedings of the Third International Workshop on Paraphrasing (IWP2005)*.

Zi-Yi Dou, Keyi Yu, and Antonios Anastasopoulos. 2019. Investigating meta-learning algorithms for low-resource natural language understanding tasks. In *Proceedings of the 2019 Conference on Empirical Methods in Natural Language Processing and the 9th International Joint Conference on Natural Language Processing (EMNLP-IJCNLP)*, pages 1192–1197, Hong Kong, China. Association for Computational Linguistics.

Chelsea Finn, Pieter Abbeel, and Sergey Levine. 2017. Model-agnostic meta-learning for fast adaptation of deep networks. In *Proceedings of the 34th International Conference on Machine Learning*, volume 70 of *Proceedings of Machine Learning Research*, pages 1126–1135. PMLR.

Tianyu Gao, Adam Fisch, and Danqi Chen. 2020. Making pre-trained language models better few-shot learners.

Danilo Giampiccolo, Hoa Trang Dang, Bernardo Magnini, Ido Dagan, Elena Cabrio, and William B. Dolan. 2008. The fourth pascal recognizing textual entailment challenge. In *Text Analysis Conference*.

Xavier Glorot and Yoshua Bengio. 2010. Understanding the difficulty of training deep feedforward neural networks. In *Proceedings of the Thirteenth International Conference on Artificial Intelligence and Statistics*, volume 9 of *Proceedings of Machine Learning Research*, pages 249–256, Chia Laguna Resort, Sardinia, Italy. PMLR.

Nithin Holla, Pushkar Mishra, Helen Yannakoudakis, and Ekaterina Shutova. 2020. Learning to learn to disambiguate: Meta-learning for few-shot word sense disambiguation. In *Findings of the Association for Computational Linguistics: EMNLP 2020*, pages 4517–4533, Online. Association for Computational Linguistics.

Edward J Hu, yelong shen, Phillip Wallis, Zeyuan Allen-Zhu, Yuanzhi Li, Shean Wang, Lu Wang, and Weizhu Chen. 2022. LoRA: Low-rank adaptation of large language models. In *International Conference on Learning Representations*.

Boonnithi Jiaramaneepinit, Thodsaporn Chay-intr, Kotaro Funakoshi, and Manabu Okumura. 2024. Extreme fine-tuning: A novel and fast fine-tuning approach for text classification. In *Proceedings of the 18th Conference of the European Chapter of the Association for Computational Linguistics (Volume 2: Short Papers)*, pages 368–379, St. Julian's, Malta. Association for Computational Linguistics.

Tushar Khot, Ashish Sabharwal, and Peter Clark. 2018. Scitail: A textual entailment dataset from science question answering. In *AAAI*.

Taesup Kim, Jaesik Yoon, Ousmane Dia, Sungwoong Kim, Yoshua Bengio, and Sungjin Ahn. 2018. Bayesian model-agnostic meta-learning.

Gregory Koch, Richard Zemel, and Ruslan Salakhutdinov. 2015. Siamese neural networks for one-shot image recognition. In *ICML deep learning workshop*, volume 2. Lille.

Sotiris Kotitsas, Panagiotis Kounoudis, Eleni Koutli, and Haris Papageorgiou. 2024. Leveraging fine-tuned large language models with LoRA for effective claim, claimer, and claim object detection. In *Proceedings of the 18th Conference of the European Chapter of the Association for Computational Linguistics (Volume 1: Long Papers)*, pages 2540–2554, St. Julian's, Malta. Association for Computational Linguistics.

Brenden M. Lake, Ruslan Salakhutdinov, and Joshua B. Tenenbaum. 2015. Human-level concept learning through probabilistic program induction. *Science*, 350(6266):1332–1338.

Balaji Lakshminarayanan, Alexander Pritzel, and Charles Blundell. 2017. Simple and scalable predictive uncertainty estimation using deep ensembles. In *Advances in Neural Information Processing Systems*, volume 30. Curran Associates, Inc.

Anna Langedijk, Verna Dankers, Phillip Lippe, Sander Bos, Bryan Cardenas Guevara, Helen Yannakoudakis, and Ekaterina Shutova. 2022. Meta-learning for fast cross-lingual adaptation in dependency parsing. In *Proceedings of the 60th Annual Meeting of the Association for Computational Linguistics (Volume 1: Long Papers)*, pages 8503–8520, Dublin, Ireland. Association for Computational Linguistics.

Stefan Lee, Senthil Purushwalkam, Michael Cogswell, David Crandall, and Dhruv Batra. 2015. Why m heads are better than one: Training a diverse ensemble of deep networks.

Brian Lester, Rami Al-Rfou, and Noah Constant. 2021. The power of scale for parameter-efficient prompt tuning.

Jiachang Liu, Dinghan Shen, Yizhe Zhang, Bill Dolan, Lawrence Carin, and Weizhu Chen. 2022. What makes good in-context examples for GPT-3? In *Proceedings of Deep Learning Inside Out (DeeLIO 2022): The 3rd Workshop on Knowledge Extraction and Integration for Deep Learning Architectures*, pages 100–114, Dublin, Ireland and Online. Association for Computational Linguistics.

Jingjing Liu, Panupong Pasupat, Scott Cyphers, and Jim Glass. 2013. Asgard: A portable architecture for multilingual dialogue systems. In *2013 IEEE International Conference on Acoustics, Speech and Signal Processing*, pages 8386–8390.

Pengfei Liu, Weizhe Yuan, Jinlan Fu, Zhengbao Jiang, Hiroaki Hayashi, and Graham Neubig. 2021. Pretrain, prompt, and predict: A systematic survey of prompting methods in natural language processing. *ACM Computing Surveys*, 55:1 – 35.

Ilya Loshchilov and Frank Hutter. 2017a. Decoupled weight decay regularization.

Ilya Loshchilov and Frank Hutter. 2017b. SGDR: stochastic gradient descent with warm restarts. In *5th International Conference on Learning Representations, ICLR 2017, Toulon, France, April 24-26, 2017, Conference Track Proceedings*. OpenReview.net.

Sewon Min, Xinxi Lyu, Ari Holtzman, Mikel Artetxe, Mike Lewis, Hannaneh Hajishirzi, and Luke Zettlemoyer. 2022. Rethinking the role of demonstrations: What makes in-context learning work? In *Proceedings of the 2022 Conference on Empirical Methods in Natural Language Processing*, pages 11048–11064, Abu Dhabi, United Arab Emirates. Association for Computational Linguistics.

Takeru Miyato, Andrew M. Dai, and Ian Goodfellow. 2016. Adversarial training methods for semi-supervised text classification.

MOSEK ApS. 2019. *The MOSEK optimization toolbox for MATLAB manual. Version 9.3.*

Aaron Mueller, Kanika Narang, Lambert Mathias, Qifan Wang, and Hamed Firooz. 2023. Meta-training with demonstration retrieval for efficient few-shot learning. In *Findings of the Association for Computational Linguistics: ACL 2023*, pages 6049–6064, Toronto, Canada. Association for Computational Linguistics.

Alex Nichol, Joshua Achiam, and John Schulman. 2018. On first-order meta-learning algorithms.

Farhad Nooralahzadeh, Giannis Bekoulis, Johannes Bjerva, and Isabelle Augenstein. 2020. Zero-shot cross-lingual transfer with meta learning.

Abiola Obamuyide and Andreas Vlachos. 2019a. Meta-learning improves lifelong relation extraction. In *Proceedings of the 4th Workshop on Representation Learning for NLP (RepL4NLP-2019)*, pages 224–229, Florence, Italy. Association for Computational Linguistics.

Abiola Obamuyide and Andreas Vlachos. 2019b. Model-agnostic meta-learning for relation classification with limited supervision. In *Proceedings of the 57th Annual Meeting of the Association for Computational Linguistics*, pages 5873–5879, Florence, Italy. Association for Computational Linguistics.

OpenAI. 2024. Gpt-4 technical report.

Alec Radford, Jeff Wu, Rewon Child, David Luan, Dario Amodei, and Ilya Sutskever. 2019. Language models are unsupervised multitask learners.

Sachin Ravi and Hugo Larochelle. 2017. Optimization as a model for few-shot learning. In *International Conference on Learning Representations*.

Sashank J. Reddi, Satyen Kale, and Sanjiv Kumar. 2018. On the convergence of adam and beyond. In *International Conference on Learning Representations*.

Victor Sanh, Albert Webson, Colin Raffel, Stephen H. Bach, Lintang Sutawika, Zaid Alyafeai, Antoine Chaffin, Arnaud Stiegler, Teven Le Scao, Arun Raja, Manan Dey, M Saiful Bari, Canwen Xu, Urmish Thakker, Shanya Sharma Sharma, Eliza Szczechla, Taewoon Kim, Gunjan Chhablani, Nihal Nayak, Debajyoti Datta, Jonathan Chang, Mike Tian-Jian Jiang, Han Wang, Matteo Manica, Sheng Shen, Zheng Xin Yong, Harshit Pandey, Rachel Bawden, Thomas Wang, Trishala Neeraj, Jos Rozen, Abheesht Sharma, Andrea Santilli, Thibault Fevry, Jason Alan Fries, Ryan Teehan, Tali Bers, Stella Biderman, Leo Gao, Thomas Wolf, and Alexander M. Rush. 2021. Multitask prompted training enables zero-shot task generalization.

Timo Schick and Hinrich Schütze. 2020. It's not just size that matters: Small language models are also few-shot learners.

Jurgen Schmidhuber. 1987. Evolutionary principles in self-referential learning. *On learning how to learn: The meta-meta-... hook.) Diploma thesis, Institut f. Informatik, Tech. Univ. Munich*, 1(2).

Jake Snell, Kevin Swersky, and Richard S. Zemel. 2017. Prototypical networks for few-shot learning.

Richard Socher, Alex Perelygin, Jean Wu, Jason Chuang, Christopher D. Manning, Andrew Ng, and Christopher Potts. 2013. Recursive deep models for semantic compositionality over a sentiment treebank. In *Proceedings of the 2013 Conference on Empirical Methods in Natural Language Processing*, pages 1631–1642, Seattle, Washington, USA. Association for Computational Linguistics.

Ilia Sucholutsky, Nam-Hwui Kim, Ryan P. Browne, and Matthias Schonlau. 2021. One line to rule them all: Generating LO-shot soft-label prototypes. In *2021 International Joint Conference on Neural Networks (IJCNN)*. IEEE.

Ilia Sucholutsky and Matthias Schonlau. 2021. 'less than one'-shot learning: Learning n classes from m < n samples. *Proceedings of the AAAI Conference on Artificial Intelligence*, 35(11):9739–9746.

Chi Sun, Xipeng Qiu, Yige Xu, and Xuanjing Huang. 2020. How to fine-tune bert for text classification?

Simeng Sun, Yang Liu, Shuohang Wang, Dan Iter, Chenguang Zhu, and Mohit Iyyer. 2024. PEARL: Prompting large language models to plan and execute actions over long documents. In *Proceedings of the 18th Conference of the European Chapter of the Association for Computational Linguistics (Volume 1: Long Papers)*, pages 469–486, St. Julian's, Malta. Association for Computational Linguistics.

Sebastian Thrun and Lorien Pratt. 1998. Learning to learn: Introduction and overview. In *Learning to learn*, pages 3–17. Springer.

Erik F. Tjong Kim Sang and Fien De Meulder. 2003. Introduction to the CoNLL-2003 shared task: Language-independent named entity recognition. In *Proceedings of the Seventh Conference on Natural Language Learning at HLT-NAACL 2003*, pages 142–147.

Hugo Touvron, Thibaut Lavril, Gautier Izacard, Xavier Martinet, Marie-Anne Lachaux, Timothée Lacroix, Baptiste Rozière, Naman Goyal, Eric Hambro, Faisal Azhar, Aurelien Rodriguez, Armand Joulin, Edouard Grave, and Guillaume Lample. 2023. Llama: Open and efficient foundation language models.

Niels van der Heijden, Helen Yannakoudakis, Pushkar Mishra, and Ekaterina Shutova. 2021. Multilingual and cross-lingual document classification: A meta-learning approach. In *Proceedings of the 16th Conference of the European Chapter of the Association for Computational Linguistics: Main Volume*, pages 1966–1976, Online. Association for Computational Linguistics.

Alex Wang, Amanpreet Singh, Julian Michael, Felix Hill, Omer Levy, and Samuel Bowman. 2018. GLUE: A multi-task benchmark and analysis platform for natural language understanding. In *Proceedings of the 2018 EMNLP Workshop BlackboxNLP: Analyzing and Interpreting Neural Networks for NLP*, pages 353–355, Brussels, Belgium. Association for Computational Linguistics.

Zhiguo Wang, Wael Hamza, and Radu Florian. 2017. Bilateral multi-perspective matching for natural language sentences.

Zirui Wang, Zachary C. Lipton, and Yulia Tsvetkov. 2020. On negative interference in multilingual models: Findings and a meta-learning treatment. In *Proceedings of the 2020 Conference on Empirical Methods in Natural Language Processing (EMNLP)*, pages 4438–4450, Online. Association for Computational Linguistics.

Alex Warstadt, Amanpreet Singh, and Samuel R Bowman. 2018. Neural network acceptability judgments. *arXiv preprint arXiv:1805.12471*.

Adina Williams, Nikita Nangia, and Samuel Bowman. 2018. A broad-coverage challenge corpus for sentence understanding through inference. In *Proceedings of the 2018 Conference of the North American Chapter of the Association for Computational Linguistics: Human Language Technologies, Volume 1 (Long Papers)*, pages 1112–1122, New Orleans, Louisiana. Association for Computational Linguistics.

Andrew G Wilson and Pavel Izmailov. 2020. Bayesian deep learning and a probabilistic perspective of generalization. In *Advances in Neural Information Processing Systems*, volume 33, pages 4697–4708. Curran Associates, Inc.

Qizhe Xie, Zihang Dai, Eduard Hovy, Minh-Thang Luong, and Quoc V. Le. 2019. Unsupervised data augmentation for consistency training.

Adam Yang, Maxime Robeyns, Xi Wang, and Laurence Aitchison. 2024. Bayesian low-rank adaptation for large language models. In *Socially Responsible Language Modelling Research*.

Linyi Yang, Yaoxian Song, Xuan Ren, Chenyang Lyu, Yidong Wang, Jingming Zhuo, Lingqiao Liu, Jindong Wang, Jennifer Foster, and Yue Zhang. 2023. Out-of-distribution generalization in natural language processing: Past, present, and future. In *The 2023 Conference on Empirical Methods in Natural Language Processing*.

Zihao Zhao, Eric Wallace, Shi Feng, Dan Klein, and Sameer Singh. 2021. Calibrate before use: Improving few-shot performance of language models. In *Proceedings of the 38th International Conference on Machine Learning*, volume 139 of *Proceedings of Machine Learning Research*, pages 12697–12706. PMLR.

Kun Zhou, Yifan Li, Xin Zhao, and Ji-Rong Wen. 2024. Diffusion-NAT: Self-prompting discrete diffusion for non-autoregressive text generation. In *Proceedings of the 18th Conference of the European Chapter of the Association for Computational Linguistics (Volume 1: Long Papers)*, pages 1438–1451, St. Julian's, Malta. Association for Computational Linguistics.

Yichu Zhou and Vivek Srikumar. 2022. A closer look at how fine-tuning changes BERT. In *Proceedings of the 60th Annual Meeting of the Association for Computational Linguistics (Volume 1: Long Papers)*, pages 1046–1061, Dublin, Ireland. Association for Computational Linguistics.

A Appendix

A.1 Deriving soft-label prototypes using constraintSLP

Finding lines connecting all centroids

In Figure 3a, we present an example set of lines connecting all class centroids. For further details on recursive regression, we refer the reader to Sucholutsky et al. (2021).

Deriving soft-label prototypes by optimising for linear constraints

Example soft-label prototypes which are "set" at the ends of each line are shown in Figure 3b.

Classification with constraintSLP: A toy example

Figure 4 presents an example classification with soft-label prototypes. Given the class centroids for *blue*, *green* and *yellow* are located at $(0, 0)$, $(1.5, 0)$ and $(3, 0)$ respectively, two soft-label prototypes are defined by a line connecting *yellow* and *blue*, and are thus located at $(3, 0)$ and $(0, 0)$ respectively. The soft labels in Figure 4a contain

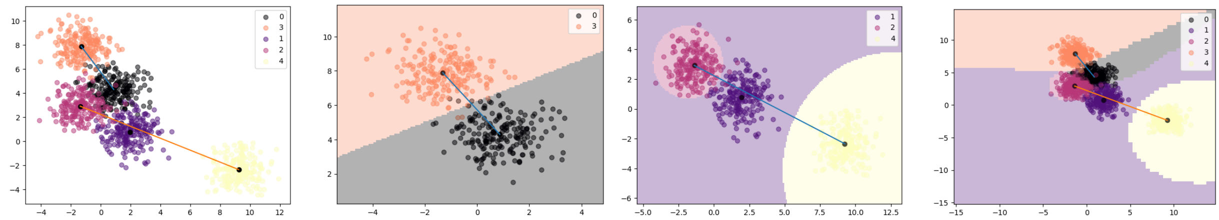

a Computing lines

b Generating soft-label prototypes

c The decision landscape

Figure 3: Generating and classifying data with soft-label prototypes.

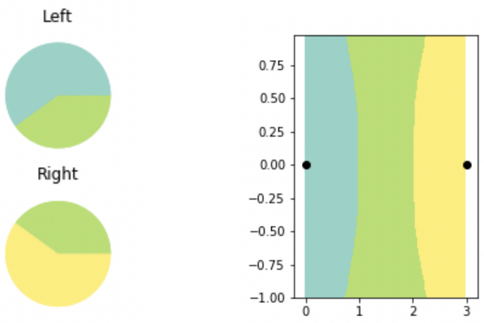

a

b

Figure 4: Classification example with constraintSLP (figure from Sucholutsky and Schonlau (2021)).

the per-class probability distribution derived by the constraintSLP method; for example, $p(x = blue) = 0.6$ and $p(x = green) = 0.4$ for the left prototype, and $p(x = green) = 0.4$ and $p(x = yellow) = 0.6$ for the right prototype. When a new test instance x located at $(1.5, 0.8)$ is presented, we make predictions as follows: we find the nearest line to x and consider its distance from the two prototypes at the ends of the line and multiply the class distribution of each prototype by the inverse distance as per Eq. 1.

Since x is equidistant from both prototypes, the distance between the x and each prototype is 1.5. Therefore, the values for *blue* and *yellow* (given both soft-label prototypes) become $soft\_label(x = blue) = \frac{0.6}{1.5} + \frac{0}{1.5} = 0.4$ and $soft\_label(x = yellow) = \frac{0}{1.5} + \frac{0.6}{1.5} = 0.4$ respectively. In contrast, for *green*, which is directly informed by both prototypes (i.e., no zero values in the numerator), the probability distribution becomes $soft\_label(x = green) = \frac{0.4}{1.5} + \frac{0.4}{1.5} = 0.53$. Therefore x is classified as green. This decision boundary can be seen in Figure 4b.

A.2 Meta-learning

For encoder-based models, meta-learning has emerged as a viable methodology for few-shot learning. In the meta-learning paradigm, the training and test sets, referred to as $\mathcal{D}_{\text{meta-train}}$ and $\mathcal{D}_{\text{meta-test}}$, are split into episodes. Each episode encompasses a task $\mathcal{T}_{\text{i}}$ and consists of a support set $\mathcal{D}^{(i)}{}_{\text{support}}$ and a query set $\mathcal{D}^{(i)}{}_{\text{query}}$. Meta-learning algorithms initially fit the model on the support set of the episode (inner-loop optimisation) and then achieve generalisation across episodes by optimising performance on the query sets of the episodes (outer-loop optimisation). For evaluation, the model is first fine-tuned on the support set and then evaluated on the query set for each task $\mathcal{T}_{\text{i}}$ $\in \mathcal{D}_{\text{meta-test}}$. We describe the process algorithmically in Algorithm 2 and describe the *MetaUpdate* process for different algorithms subsequently.

Algorithm 2: Meta-learning

```
$\alpha, \beta \leftarrow$ learning rates
Sample batch of tasks $\{T_i\} \sim p(T)$
Initialise $\theta'_{\text{i}} \leftarrow \theta$
**for** $T_i \sim p(T)$ **do**
    Partition $T_i$ into $D_i^s$ and $D_i^q$
    $\theta'_{\text{i}} \leftarrow \theta - \alpha \nabla_\theta \mathcal{L}^s_{\mathcal{D}_i}(f_\theta)$ for $k$ steps
**end**
$\theta \leftarrow$ MetaUpdate$(\theta_i, D_i^q, \beta)$
```

Model Agnostic Meta-Learning MAML (Finn et al., 2017) is an *optimisation-based* meta-learning approach which incorporates generalisability across tasks in its cost function. The task loss $\mathcal{L}^q_{\mathcal{T}_i}$ is computed on the query examples in each episode, using this task-specific model. The initial model parameters θ are then updated so as to minimize the sum of the losses of all tasks in a batch, leading to improved generalisation across tasks. The *MetaUpdate* step is thus defined as

$$\theta \leftarrow \theta - \beta \, \nabla_\theta \sum_{\mathcal{T}_i \sim p(\mathcal{T})} \mathcal{L}^q_{\mathcal{D}_i}(f_{\theta'_i})$$

Note that the *MetaUpdate* expression calculates the gradients of each θ_i with respect to θ, thus necessitating the computation of second-order gradients. To ease computation, we use a first-order approximation of MAML (FOMAML) wherein the gradients of each θ_i are calculated with respect to θ_i and reduce the *MetaUpdate* term to

$$\theta \leftarrow \theta - \beta \, \nabla_{\theta_i} \sum_{\mathcal{T}_i \sim p(\mathcal{T})} \mathcal{L}^q_{\mathcal{D}_i}(f_{\theta'_i})$$

LEOPARD Bansal et al. (2020a) employ meta-learning for diverse NLP tasks in an approach inspired from MAML which integrates a text encoder model with a meta-learned parameter generator to tailor task-specific initialisations for the classification head. Their inner-loop update learns the parameter generator for the task, adapts task-specific model parameters and the *MetaUpdate* step adapts model parameters as done in MAML. They show that their method, LEOPARD, outperforms multi-task trained models as well as a range of other meta-learning methods.

Reptile This meta-learning algorithm, introduced by Nichol et al. (2018), is computationally simple compared to MAML and LEOPARD - the *MetaUpdate* step simply moves the model parameters towards inner-loop fine-tuned model parameters, thus assuming the form:

$$\theta \leftarrow \theta + \beta \frac{1}{|\{T_i\}|} \sum_{T_i \sim p(T)} (\theta_i - \theta)$$

Despite it's simplicity, it reports strong performance on a variety of few-shot learning tasks (Dou et al., 2019).

Prototypical Networks Unlike optimisation-driven meta-learning methods, Prototypical Networks (Snell et al., 2017) is a metric-based meta-learning method that uses an embedding function f_θ to encode training support samples and compute a high-dimensional vector μ_c that is the arithmetic mean of the training data points of class c. It then uses a distance function d to compute the similarity between a query instance x and the mean vector of each class to get the class distribution as:

$$\begin{aligned} p(y = c|x) &= softmax(-d(f_\theta(x), \mu_c)) \\ &= \frac{exp(-d(f_\theta(x), \mu_c))}{\sum_{c' \in C} exp(-d(f_\theta(x), \mu'_c))} \end{aligned}$$

Model optimisation is done using the loss function $J(\theta) = -log(p(y = c^*|x, \theta))$.

A.3 Analysis of soft-labels derived from linear constraints: constraintSLP

Theorem A.1. *The soft-label value of each class within a single soft-label prototype generated using constraintSLP is inversely proportional to its distance from the soft-label prototype along the line connecting all classes captured by it.*

Proof of Theorem A.1 (Informal) Consider a line l connecting three class centroids (while we focus on a three class system, the conclusions generalise to $n > 3$ classes too). The class centroids are represented by A, B and C. The soft-label prototypes at ends A and C contain the values $[a_1, a_2, a_3]$ and $[c_1, c_2, c_3]$ respectively. Consider a support example $x \in A$ at a distance d_a and d_b from A and C respectively. Directly using the constraints in Algorithm 4 of Sucholutsky et al. (2021), we state that the influence of A (i.e., the distance-weighted sum of the soft-labels at x) should be more than the sum of the influence of the other two classes. Thus, we need to maximise:

$$\frac{a_1}{d_a} + \frac{c_1}{d_b} > \left(\frac{a_2}{d_a} + \frac{c_2}{d_b}\right) + \left(\frac{a_3}{d_a} + \frac{c_3}{d_b}\right) \qquad (2)$$

As we move x further towards A, $d_a \to 0$ and the influence of $[a_1/d_1, a_2/d_2, a_3/d_3]$ increases thus $\sum_{i=2}^{i=3} c_i/d_b <<< \sum_{i=2}^{i=3} a_i/d_a$. Therefore we have the approximation:

$$\frac{a_1}{d_a} > \frac{a_2}{d_a} + \frac{a_3}{d_a} \implies a_1 > a_2 + a_3 \qquad (3)$$

If we take a support example $x \in C$, by symmetry as x is moved towards C, $d_b \to 0$, we can also write:

$$\frac{c_3}{d_b} > \frac{c_2}{d_b} + \frac{c_1}{d_b} \implies c_3 > c_2 + c_1 \qquad (4)$$

Furthermore, consider a point x in the middle of l equidistant from A and C (by a distance d) – such a point will always be classified as $x \in B$. Thus, the influence of B should be higher than both A and C. Thus we have:

$$\begin{aligned} &\frac{a_2}{d} + \frac{c_2}{d} > \frac{a_1}{d} + \frac{c_1}{d} \quad \& \quad \frac{a_2}{d} + \frac{c_2}{d} > \frac{a_3}{d} + \frac{c_3}{d} \\ &\implies a_2 + c_2 > a_1 + c_1 \quad \& \quad a_2 + c_2 > a_3 + c_3 \end{aligned}$$

From Equation 3 and Equation 4 we can replace a_1 and c_3 and get:

$$a_2 + c_2 > a_2 + a_3 + c_1 \implies c_2 > c_1$$
$$a_2 + c_2 > a_3 + c_2 + c_1 \implies a_2 > a_3$$

Therefore, we have:

$$a_1 > a_2 > a_3 \quad \& \quad c_3 > c_2 > c_1$$

This is an intuitive result as the soft-label value of each class decreases as the distance of the class centroid increases from the prototype location – the class nearest to the prototype has the highest soft-label value and the class furthest away has the lowest soft-label value.

Recall that $\sum_{i=1}^{3} a_i = 1$ and $\sum_{i=1}^{3} c_i = 1$ and $a_i, c_i \geq 0 \ \forall i = \{1, 2, 3\}$ otherwise the optimisation problem becomes unbounded. Therefore, the ranges of values for $[a_1, a_2, a_3]$ and $[c_1, c_2, c_3]$ are:

$$a_3 \in [0, a_2),\ a_2 \in (a_3, a_1),\ a_1 \in (a_2, 1]$$
$$c_3 \in (c_2, 1],\ c_2 \in (c_1, c_3),\ c_1 \in [0, c_2)$$

Using Algorithm 4 in Sucholutsky et al. (2021), we see that there are multiple constraints for a_1 and a_2 which require them to be maximised, but there are none for a_3. Thus, to maximise Equation 3, a_3 adjusts to the minimum value it can get:

$$a_3 = min(0, a_2) = \epsilon \simeq 0$$

By symmetry, we can also conclude that:

$$c_1 = min(0, c_2) = \epsilon \simeq 0$$

These approximations are also generalisable to multiple classes connected by a line, for example, if a line connects only two centroids, the soft-labels at each end are derived as $[0, 1]$ and $[1, 0]$ - the same as a “hard" label. These findings are substantiated experimentally in Table 2 where we examine the soft-labels generated by DeepSLP and constraintSLP using a few-shot training support set of the task *airline* with 8 examples per class – the constraintSLP soft label corresponding to the furthest class from the prototype location drops to almost zero compared to other soft label values. On the other hand, DeepSLP prevents overfitting on the nearest classes and produces a more generalised distribution of soft-labels. This is a trend generally observed in other tasks and classes as well. We further use this theorem to prove the main theorem given by Theorem A.2.

Theorem A.2. *The constant soft-labels in constraintSLP do not always select the closest class centroid to a test point.*

#	**constraintSLP**	**DeepSLP(x)**
1	$5.6422e-01$	$9.7887e-01$
	$4.3577e-01$	$2.0995e-02$
	$9.7973e-16$	$1.3500e-04$
2	$5.3090e-13$	$2.5240e-02$
	$4.3212e-01$	$9.7475e-01$
	$5.6787e-01$	$1.0000e-05$

Table 2: Soft labels derived using constraintSLP and DeepSLP. # denotes the index of the soft-label prototype lying on the line. Soft labels are constant for constraintSLP, however, they are a function of input point x for DeepSLP, thus allowing more flexibility.

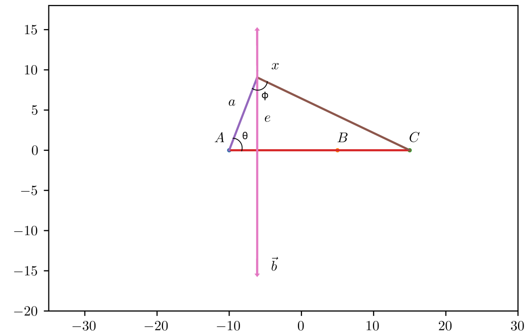

Figure 5: Schematic diagram for ascertaining θ with class centroids $A = (-10, 0)$, $B = (5, 0)$ and $C = (15, 0)$.

Proof of Theorem A.2 (Informal) Furthermore, consider a line b perpendicular to l – it intersects l between A and B. We select θ such that $\phi = \pi/2$. We denote the complete setup diagrammatically in Figure 5.

Consider the distance weighted influences at x for class A. We have the influence as $\frac{a_1 sin\theta}{e} + \frac{c_1 cos\theta}{e} = \frac{a_1 sin\theta}{e}$ as $c_1 \simeq 0$. Similarly, for class B, we have the weighted influence as $\frac{a_2 sin\theta}{e} + \frac{c_2 cos\theta}{e}$. To calculate values of θ where the weighted influence of B is more than the weighted influence of A, we get:

$$\frac{a_2 sin\theta}{e} + \frac{c_2 cos\theta}{e} > \frac{a_1 sin\theta}{e}$$
$$\implies a_2 sin\theta + c_2 cos\theta > a_1 sin\theta$$
$$\implies c_2 cos\theta - (a_1 - a_2) sin\theta > 0$$
$$\implies \frac{c_2 cos\theta - (a_1 - a_2) sin\theta}{\sqrt{c_2^2 + (a_1 - a_2)^2}} > 0$$
$$\implies cos(\theta + \alpha) > 0$$

where $\alpha = tan^{-1}\left(\frac{a_1 - a_2}{c_2}\right)$. Since $cos(\theta + \alpha) > 0$

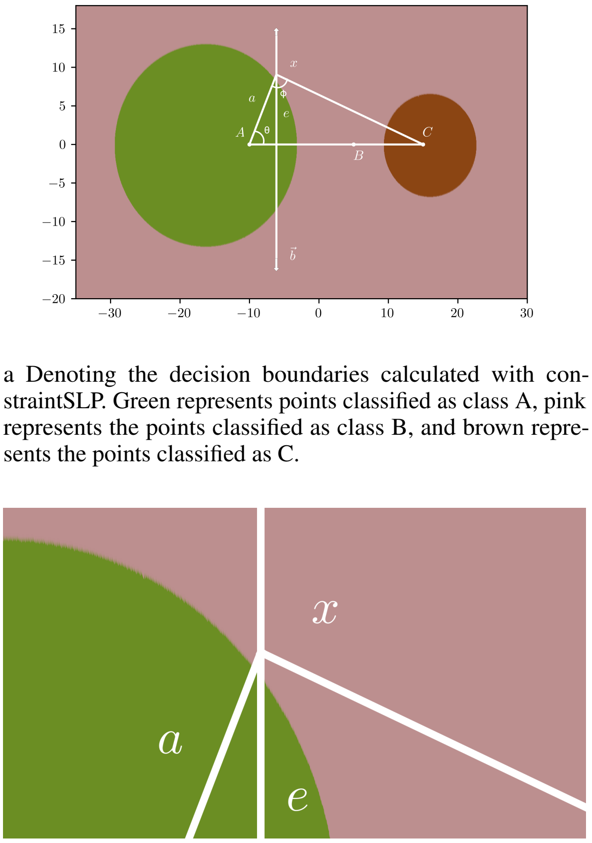

a Denoting the decision boundaries calculated with constraintSLP. Green represents points classified as class A, pink represents the points classified as class B, and brown represents the points classified as C.

b Zooming in at point x. We can see that it is classified as B.

Figure 6: The soft-labels of the linear constraint system at A and C using constraintSLP are calculated as $[0.5963, 0.4036, 0.0001]$ and $[0.0001, 0.4495, 0.5504]$. We also get $\theta = 66.84°$. Using these soft-labels, we calculate the decision boundaries for points in this area. We use θ to calculate the coordinates of x. Zooming in, we can visually inspect that x is classified to class B. For x, the Euclidean distance of x from A and B is 9.847 and 14.338 respectively. From the figure, we can see that constraintSLP classifies x as B even though the Euclidean distance of x from A is shorter.

we have $(\theta + \alpha) \in (-\pi/2, \pi/2)$ and since $\theta > 0$, thus for $\theta \in [0, \pi/2 - \alpha)$, the weighted influence of B is more than the weighted influence of A.

However, it is worth observing the result for θ derived above can contain points closer to A (using Euclidean distance) which are *actually* classified as B. We can easily demonstrate this with a counter example explained in Figure 6.

Therefore, for points closer to A compared to B using an Euclidean measure, constraintSLP can still return a higher value for the influence at B compared to A. This adversely affects performance in classifiers where we rely on selection of the closest class centroid for classification – such as 1-NN, Prototypical Networks, and constraintSLP – and we believe this is the reason behind the poor performance of constraintSLP for cases where the total classes is greater than two.

Algorithm 3: Inner-loop training of MetaSLP

```
$\mathcal{T}_i \leftarrow$ meta-training task
$\mathcal{L} \leftarrow$ line connecting both centroids of a task
$\alpha \leftarrow$ inner-loop learning rate
$\mathcal{S} \leftarrow$ inner-loop optimisation steps
Initialise $g_1 x(x)$ and $g_2(x)$ randomly
while $s < \mathcal{S}$ do
    Sample support examples $X^s$ for $\mathcal{T}_i$
    Calculate locations of each soft-label prototype in $\mathcal{L}$
    Use Equation 1 to classify $x \in X^s$
    Calculate $\nabla \mathcal{L}_{\mathcal{T}_i}(f_\theta(x), g_1(x), g_2(x))$
    Scale $\nabla_\phi \mathcal{L}_{\mathcal{T}_i}(g_1(x))$ and $\nabla_\omega \mathcal{L}_{\mathcal{T}_i}(g_2(x))$ by the distances from the soft-label prototypes
    $\theta'_i \leftarrow \theta - \alpha \nabla_\theta \mathcal{L}_{\mathcal{T}_i}(f_\theta(x))$
    $\theta'_{1_i} \leftarrow \theta_1 - \alpha \nabla_\phi \mathcal{L}_{\mathcal{T}_i}(g_1(x))$
    $\theta'_{2_i} \leftarrow \theta_2 - \alpha \nabla_\omega \mathcal{L}_{\mathcal{T}_i}(g_2(x))$
end
```

A.4 Training algorithms for MetaSLP

Inner-loop training Our inner-loop training algorithm for MetaSLP is presented in Algorithm 3. The inner-loop encoder optimisation can be understood as updating the parameters of the encoder to "push" different classes away from each other and "pull" points belonging to the same class together; i.e., increase inter-class distance and decrease intra-class distance which leads to well-defined clusters per class. We present this process in Figure 7.

Outer-loop training Our outer-loop training algorithm is presented in Algorithm 4.

A.5 Meta-training details

GLUE (Wang et al., 2018) tasks and their details are provided in Table 3. These tasks include MNLI (Williams et al., 2018), SST2 (Socher et al., 2013), CoLA (Warstadt et al., 2018), MRPC (Dolan and Brockett, 2005), QQP (Wang et al., 2017), QNLI (Wang et al., 2018), RTE (Giampiccolo et al., 2008) and SNLI (Bowman et al., 2015). We employ the same tasks as Bansal et al. (2020a) to ensure direct comparability. Note that the datasets and

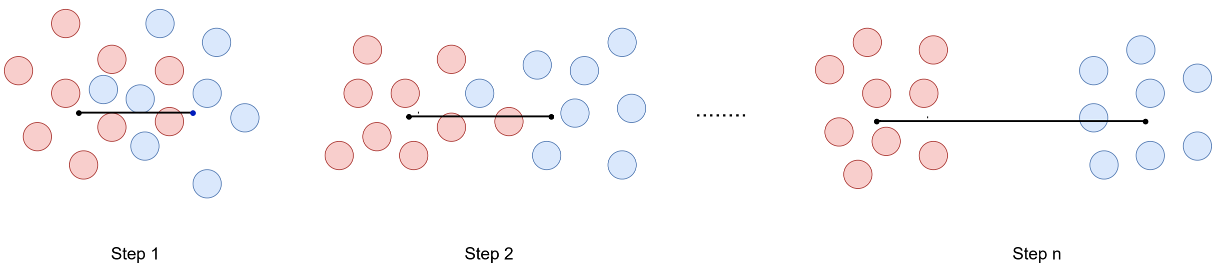

Figure 7: Inner-loop training – note that inter-class embeddings are pushed further away, and intra-class embeddings are pushed closer together across n steps. The endpoints of the line mark the location of the soft-label prototypes.

Algorithm 4: Outer-loop training of MetaSLP

```
$\mathcal{T} \leftarrow$ batch of meta-training tasks, $|\mathcal{T}| = n$
$\mathcal{M} \leftarrow$ batch of distinct inner-loop optimised models parameterised by $\theta_i$, $|\mathcal{M}| = n$
$\beta \leftarrow$ outer-loop learning rate
for $\mathcal{T}_i,\ \mathcal{M}_i \in \mathcal{T},\ \mathcal{M}$ do
    if FOMAML then
        Sample query examples $X^q$ for $\mathcal{T}_i$, $X^s \cap X^q = \Phi$
        Use Equation 1 to classify $x \in X^q$
        Calculate $\nabla_{\theta'_i}\mathcal{L}_{\mathcal{T}_i}(f_{\theta'_i}(x), g_{\phi'_i}(x), h_{\omega'_i}(x))$
        Update $\nabla_{\theta}\mathcal{L}_{\mathcal{T}_i}(f_{\theta}(x)) += \nabla_{\theta'_i}\mathcal{L}_{\mathcal{T}_i}(f_{\theta'_i}(x), g_{\phi'_i}(x), h_{\omega'_i}(x))$
    end
    if Reptile then
        Update $\nabla_{\theta}\mathcal{L}_{\mathcal{T}_i}(f_{\theta}(x)) += \theta - \theta_i$
    end
end
Update $\theta \leftarrow \theta - \frac{\beta}{n}\sum_{i=1}^{n}\nabla_{\theta}\mathcal{L}_{\mathcal{T}_i}(f_{\theta}(x))$
```

classes in GLUE are completely different from the datasets used for evaluating the model - thus the final model fine-tunes on unseen few-shot data and learns classes it has previously not encountered.

To train our model to detect the sentiment contained within phrases of a sentence by using the annotations for phrases within sentences for SST2, we append a separator token and the annotated phrase for each sentence at the end of the sentence in the form "[CLS] <sentence_1> [SEP] <sentence_2> [SEP]" and obtain the passage level embedding for training.

Dataset	Labels	Training Size	Validation Size	Test Size
CoLA	2	8551	1042	-
MRPC	2	3669	409	-
QNLI	2	104744	5464	-
QQP	2	363847	40431	-
RTE	2	2491	278	-
SNLI	3	549368	9843	-
SST-2	2	67350	873	-
MNLI	3	392703	19649	-

Table 3: Details of GLUE tasks used for meta-training.

A.6 Hyperparameters

Generating lines The hyperparameters used to generate lines are: (a) ϵ, which is a control factor used to denote the maximum tolerance between a centroid and the line assigned to it using Euclidean distance—we use a tolerance value of $1e-1$; and (b) l, which denotes the maximum number of lines used to connect all centroids. We experiment with a range of values ($l \in \{0.25n, 0.5n, 0.75n, n-1\}$, where n is the number of centroids), but find $l = \lceil n/2 \rceil$ to give the best accuracy on the validation data with the minimum number of lines required.[4]

DeepSLP For DeepSLP, we find that more epochs are needed to train models with a higher number of soft labels (i.e., a higher number of classes in the output of the classifier head) - essentially, 3 classes fitted on a line need more epochs compared to 2 classes fitted on a line. We use *AdamW* (Loshchilov and Hutter, 2017a) as our optimiser and perform hyperparameter tuning on the validation set. We only need a few epochs (5 to 10) to generalise well depending on the training task. We fix a random seed, train our models and evaluate performance on the test tasks. We repeat

[4] The right choice of hyperparameters is key as the optimisation process fails when it is not possible to connect n centroids with l lines.

Parameter	Search Space	MetaSLP$_{\text{REPTILE}}$	MetaSLP$_{\text{FOMAML}}$	Reptile
Tunable layers (v)	$[1, 2, 3, 4]$	4	4	4
K-shot	$[8, 16, 32]$	16	16	16
Batch size	$[8, 16, 32]$	16	16	16
Steps	$[3, 5, 7]$	5	5	5
α_f	$[5e-3, 1e-3, 1e-4]$	$5e-3$	Learnable	$1e-3$
$\alpha_g,\ \alpha_h$	$[5e-3, 1e-3, 1e-4, 1e-2]$	$5e-3$	Learnable	$1e-3$
Nesterov	$[True, False]$	$True$	$True$	$True$
Momentum	$[0.5, 0.7, 0.9]$	0.9	0.9	$True$
β_{initial}	$[1e-5, 2e-5, 5e-5]$	$5e-5$	$2e-5$	$1e-5$
β_{final}	$[1e-5, 2e-5, 5e-6]$	$2e-5$	$2e-5$	$1e-5$
Task sampling	[*square root, uniform*]	*square root*	*square root*	*square root*

Table 4: Meta-training hyperparameters.

this process across three different seeds and report the mean and standard deviation. Hyperparameters for all baselines in this setting can be found online in our code repository[5].

Meta-training For inner-loop optimisation, we use SGD as an optimiser with Nesterov and a momentum factor. We use a cosine annealing learning rate scheduler (Loshchilov and Hutter, 2017b) on our outer-loop learning rate to decay the learning rate from a starting rate to an end rate without restarts across one epoch for MetaSLP$_{\text{REPTILE}}$. We use AdamW (Loshchilov and Hutter, 2017a) as our outer-loop optimiser with AMSGrad (Reddi et al., 2018). We employ early stopping and stop training if our model does not improve it's validation set accuracy over 100 batches. We use learnable inner-loop learning rates for MetaSLP$_{\text{FOMAML}}$ per parameter group for better optimisation as indicated by previous literature (Antoniou et al., 2019). All meta-training hyperparameters can be found in Appendix A.6, Table 4.

Meta-testing Similar to inner-loop optimisation at meta-training, we use SGD with Nesterov and the same optimiser hyperparameters. However, we decay the learning rate using a cosine scheduler across all fine-tuning epochs to prevent overfitting on the few-shot (support) training set per task for MetaSLP$_{\text{REPTILE}}$.

A.7 Results

The complete set of results of all models and baselines can be seen in Table 5 for the low-resource setting and DeepSLP, and Table 6 for the high-resource setting and MetaSLP.

DeepSLP Our results (Table 5) demonstrate that DeepSLP$_{\text{BERT}}$ outperforms BERT$_{\text{fine-tuned}}$ in $31/48$ tasks, constraintSLP$_{\text{BERT}}$ in $43/48$ tasks and LORA$_{\text{BERT}}$ in $45/48$ tasks, demonstrating the usefulness of soft-label prototypes and superiority over the "standard" LLM fine-tuning paradigm, as well as the simpler constraintSLP variant. constraintSLP$_{\text{BERT}}$, on the other hand, fares worse than BERT$_{\text{fine-tuned}}$ and LORA, outperforming the former in only $19/48$ tasks and the latter in $25/48$ tasks, while exhibiting high standard deviations which can be explained by Theorem A.2, as constraintSLP can behave erratically and not select the closest point to the class centroid. Overall, DeepSLP is the best performing method, demonstrating the highest accuracy in $31/48$ tasks, while being on-par with the second best model (BERT$_{\text{fine-tuned}}$) on the remaining tasks ($15/48$ tasks). Fine-tuned BERT is, overall, the next best model with $13/48$ tasks while constraintSLP achieves the best performance amongst all methods in only $1/48$ tasks. ProtoNet's comparatively lower performance can be explained by the fact that meta-learning approaches tend to require a large number of diverse and structured meta-training tasks for effective learning — thus not making them readily suited for (extreme) few-shot learning settings.

MetaSLP In Table 6, MetaSLP$_{\text{REPTILE}}$ outperforms all baselines achieving the highest performance in $33/48$ tasks. LEOPARD is the next best model with the highest performance in $11/48$ tasks. Interestingly, MetaSLP$_{\text{FOMAML}}$ does not fare as well as MetaSLP$_{\text{REPTILE}}$ and achieves the highest performance in only $1/48$ tasks while outperforms LEOPARD in only $6/48$ tasks. MetaSLP$_{\text{FOMAML}}$ nevertheless outperforms

[5] <anon-url>

MetaSLP$_{\text{REPTILE}}$ and Reptile in natural language inference tasks – demonstrating the usefulness of learnable inner-loop learning rates across multiple task distributions while meta-training.

A.8 Ensemble properties of DeepSLP

In this study, we compare and contrast DeepSLP to ensembles and draw similarities between the two, shedding further light into the effectiveness of our approach. Each prediction decision by DeepSLP is the result of two soft-label prototypes – those that lie on each end of the line nearest to a test point x. An analogy can then be drawn between the prototypes used at prediction time and those individual (albeit independent) models that are utilised by an ensemble when producing the final classification.

While DeepSLP prototypes are not independent but are rather trained jointly (and share the same encoder), in what follows, we demonstrate that they display several properties of ensemble methods, while being computationally efficient and utilising a small number of parameters. For the analyses below, we consider the tasks Airline and Disaster using an 8-shot setting and evaluate on the test data for each. However, we find the below properties to generalise across all tasks.

A.8.1 Individual vs joint prediction

In a similar way as an ensemble exhibits superior performance to the individual models it utilises, we seek to assess whether the joint utilisation of prototypes at prediction time is indeed more effective than utilising each prototype individually. To evaluate this, we measure the probability distribution of each setting on the test data using negative log-likelihood:

$$NLL(\mathbf{f}(\mathbf{x}), y) \triangleq -log(\mathbf{f}^{(\mathbf{y})}(\mathbf{x}))$$

Following Abe et al. (2022), for a strictly convex function such as NLL, we use Jensen's inequality:

$$NLL(\mathbf{F}(\mathbf{x}), y) \ \leq \ \mathbb{E}[NLL(\mathbf{f}(\mathbf{x}), y)]$$

where $F(x)$ is the ensemble and $f(x)$ are the constituent models. The idea is that the probability distribution of the ensemble fits the target distribution more closely than the corresponding expected probability distributions of its constituent models. For joint soft-label prototypes parameterised by g_1 and g_2 and located at p_1 and p_2, we have:

$$NLL\Bigg(softmax\Bigg(\frac{g_1(f(x))}{||f(x)-p_1||}) + \frac{g_2(f(x))}{||f(x)-p_2||}\Bigg), y\Bigg)$$
$$= -\sum log\Bigg(softmax\Bigg(\frac{g_1^y(f(x))}{||f(x)-p_1||}) + \frac{g_2^y(f(x))}{||f(x)-p_2||}\Bigg)\Bigg)$$

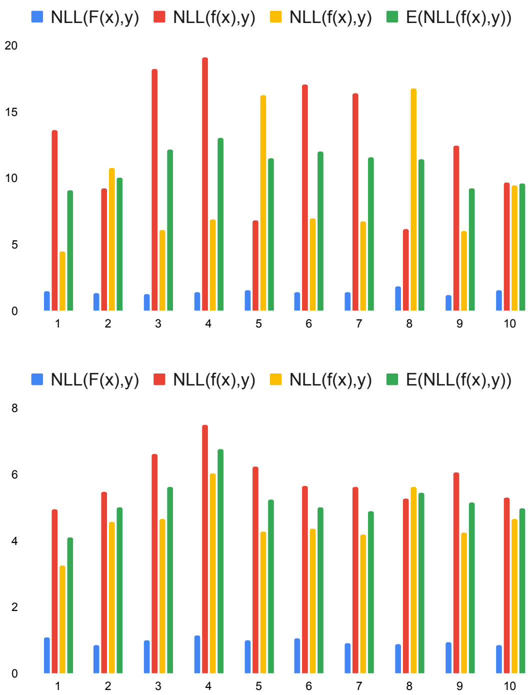

Figure 8: $NLL(\mathbf{F}(\mathbf{x}), y)$ vs. $\mathbb{E}[NLL(\mathbf{f}(\mathbf{x}), y)]$ for Disaster (top) and Airline (bottom). The i^{th} subscript refers to the i^{th} soft-label prototype.

For the individual soft-label prototypes, weighing the outputs by distance does not change the final softmax probability distribution; therefore, we can define $\mathbb{E}[NLL(\mathbf{f}(\mathbf{x}), y)]$ as their average:

$$-\frac{1}{2}\sum log(softmax(g_1^y(f(x)) + log(softmax(g_2^y(f(x))$$

We plot the negative log likelihoods for Airline and Disaster on the test set after fine-tuning each model on ten subsets of few-shot training data (as explained before in Section 4) in Figure 8 to assess whether DeepSLP exhibits this property of ensemble methods. We find that $NLL(\mathbf{F}(\mathbf{x}), y)$ is much lower than $\mathbb{E}[NLL(\mathbf{f}(\mathbf{x}), y)]$, which confirms that the joint utilisation of prototypes results in better predictions than if they were to be used individually. Our experiments confirm that this is a general trend we observe across tasks. In the following sections, we investigate the reasons behind the high values observed for $\mathbb{E}[NLL(\mathbf{f}(\mathbf{x}), y)]$, and compare the jointly trained prototypes against a strong baseline, the fine-tuned BERT baseline.

A.8.2 Jointly utilised soft-label prototypes improve diversity

Diversity in ensemble classifications refers to the difference in the probability distribution on out-of-distribution (ood) data for classifications between

Category (Classes)	**Shot**	**LORA$_{\text{BERT}}$**	**ProtoNet**	**constraintSLP$_{\text{BERT}}$**	**BERT$_{\text{fine-tuned}}$***	**DeepSLP$_{\text{BERT}}$**
Political Bias (2)	4	52.75 ± 4.33	51.15 ± 2.454	53.447 ± 3.281	54.57 ± 5.02	53.251 ± 4.042
	8	53.66 ± 4.25	56.568 ± 4.228	55.824 ± 3.725	56.15 ± 3.75	58.209 ± 5.198
	16	59.21 ± 2.27	59.183 ± 4.706	58.277 ± 4.128	60.96 ± 4.25	61.479 ± 2.974
Emotion (13)	4	7.56 ± 2.93	8.953 ± 2.052	8.662 ± 6.213	09.20 ± 3.22	9.076 ± 1.108
	8	9.02 ± 2.36	10.857 ± 3.436	8.16 ± 3.266	08.21 ± 2.12	8.041 ± 2.797
	16	10.29 ± 1.67	11.479 ± 2.96	8.115 ± 3.66	13.43 ± 2.51	10.919 ± 1.615
Sentiment Books (2)	4	51.27 ± 2.75	55.53 ± 4.097	59.89 ± 5.385	54.81 ± 3.75	58.67 ± 4.753
	8	58.16 ± 3.3	58.97 ± 4.909	64.34 ± 2.565	53.54 ± 5.17	64.78 ± 2.615
	16	59.16 ± 2.59	65.5 ± 7.026	66.36 ± 2.183	65.56 ± 4.12	67.453 ± 3.085
Rating DVD (3)	4	31.65 ± 4.91	37.665 ± 7.184	32.298 ± 16.263	32.22 ± 08.72	39.566 ± 5.086
	8	37.69 ± 3.16	37.008 ± 5.118	32.644 ± 16.016	36.35 ± 12.50	38.788 ± 4.449
	16	38.63 ± 5.52	39.123 ± 6.004	35.587 ± 17.445	42.79 ± 10.18	40.53 ± 4.375
Rating Electronics (3)	4	31.66 ± 2.94	33.696 ± 5.55	35.188 ± 16.211	39.27 ± 10.15	39.977 ± 5.959
	8	38.72 ± 5.95	37.297 ± 5.938	29.624 ± 12.876	28.74 ± 08.22	41.926 ± 3.985
	16	39.15 ± 6.6	43.825 ± 5.946	29.836 ± 12.753	45.48 ± 06.13	44.917 ± 3.164
Rating Kitchen (3)	4	36.63 ± 4.68	35.914 ± 6.678	28.253 ± 15.907	34.76 ± 11.20	39.624 ± 6.787
	8	39.69 ± 6.22	38.46 ± 11.124	24.397 ± 11.961	34.49 ± 08.72	41.081 ± 6.777
	16	38.17 ± 7.14	46.546 ± 8.394	31.926 ± 18.29	47.94 ± 08.28	45.801 ± 4.562
Political Audience (2)	4	49.75 ± 1.03	50.976 ± 1.84	51.305 ± 2.68	51.02 ± 1.72	51.741 ± 2.827
	8	54.05 ± 2.54	52.022 ± 3.964	53.104 ± 3.669	52.80 ± 2.72	54.506 ± 3.274
	16	55.39 ± 3.66	54.024 ± 3.071	53.888 ± 3.305	58.45 ± 4.98	56.956 ± 3.045
Sentiment Kitchen (2)	4	53.02 ± 1.54	55.24 ± 3.427	61.96 ± 4.594	56.93 ± 7.10	60.76 ± 4.426
	8	55.54 ± 3.47	62.28 ± 5.103	64.83 ± 3.983	57.13 ± 6.60	65.733 ± 3.198
	16	58.59 ± 4.83	66.9 ± 5.441	68.21 ± 3.298	68.88 ± 3.39	69.18 ± 2.589
Disaster (2)	4	56.02 ± 6.35	51.474 ± 8.848	52.77 ± 10.803	55.73 ± 10.29	54.252 ± 9.843
	8	57.46 ± 6.9	60.661 ± 4.991	56.888 ± 11.139	56.31 ± 09.57	61.3 ± 7.961
	16	65.79 ± 2.03	63.893 ± 6.62	65.907 ± 3.691	64.52 ± 08.93	69.28 ± 2.358
Airline (3)	4	24.36 ± 5.42	44.167 ± 10.752	36.243 ± 22.607	42.76 ± 13.50	50.987 ± 4.936
	8	52.31 ± 7.89	50.148 ± 13.429	44.972 ± 22.584	38.00 ± 17.06	55.209 ± 6.049
	16	54.1 ± 8.57	54.8 ± 10.49	29.238 ± 17.494	58.01 ± 08.23	60.247 ± 4.577
Rating Books (3)	4	34.69 ± 2.12	37.715 ± 5.801	25.562 ± 15.207	39.42 ± 07.22	42.116 ± 4.725
	8	39.36 ± 6.33	38.518 ± 5.327	34.026 ± 14.123	39.55 ± 10.01	42.156 ± 4.608
	16	41.23 ± 5.32	44.694 ± 7.797	32.509 ± 16.132	43.08 ± 11.78	46.513 ± 3.036
Political Message (9)	4	12.16 ± 1.46	13.888 ± 2.076	12.438 ± 1.799	15.64 ± 2.73	14.421 ± 1.095
	8	15.71 ± 2.04	16.155 ± 2.316	15.08 ± 2.925	13.38 ± 1.74	16.919 ± 1.756
	16	15.53 ± 2.55	18.324 ± 2.011	13.121 ± 3.294	20.67 ± 3.89	18.319 ± 1.74
Sentiment DVD (2)	4	50.77 ± 0.78	51.06 ± 3.302	56.06 ± 2.408	54.98 ± 3.96	55.003 ± 2.936
	8	52.24 ± 1.54	55.19 ± 3.298	56.98 ± 3.299	55.63 ± 4.34	57.527 ± 3.562
	16	52.6 ± 2.09	59.45 ± 3.84	58.95 ± 2.813	58.69 ± 6.08	60.76 ± 2.944
Scitail (2)	4	43.36 ± 4.74	50.227 ± 5.69	52.296 ± 4.366	58.53 ± 09.74	54.101 ± 3.759
	8	54.29 ± 5.25	54.196 ± 6.678	55.964 ± 5.705	57.93 ± 10.70	56.341 ± 5.786
	16	52.68 ± 3.0	57.744 ± 5.696	59.675 ± 4.033	65.66 ± 06.82	59.692 ± 4.227
Restaurant (8)	4	10.56 ± 1.36	18.161 ± 2.822	24.932 ± 17.102	49.37 ± 4.28	47.634 ± 5.237
	8	20.92 ± 2.4	32.146 ± 5.785	29.787 ± 9.573	49.38 ± 7.76	55.912 ± 4.494
	16	29.37 ± 4.05	40.435 ± 3.348	29.154 ± 13.537	69.24 ± 3.68	61.716 ± 2.208
CoNLL (4)	4	21.48 ± 2.71	35.438 ± 7.324	27.02 ± 7.346	50.44 ± 08.57	52.724 ± 5.84
	8	29.84 ± 3.28	44.259 ± 4.886	31.296 ± 17.487	50.06 ± 11.30	60.374 ± 3.731
	16	37.18 ± 3.32	52.116 ± 5.354	22.923 ± 7.933	74.47 ± 03.10	67.496 ± 4.551

Table 5: Classification performance (accuracy) of our methods (constraintSLP and DeepSLP) and baselines in the low-resource setting. Entries in grey indicate the best model out of all; * refers to the baseline as reported in Bansal et al. (2020a). Subscripts for constraintSLP and DeepSLP refer to the (non-fine-tuned) encoder used. Each set of results is separated by a double line. The first set of results contains intent classification tasks, the second set has a natural language inference task and the last set contains entity typing tasks.

Category (Classes)	Shot	ProtoNet	LEOPARD*	Reptile	MetaSLP$_{\text{REPTILE}}$	MetaSLP$_{\text{FOMAML}}$
Political Bias (2)	4	56.33 ± 4.37	60.49 ± 6.66	58.82 ± 4.31	60.96 ± 6.13	55.06 ± 5.9
	8	58.87 ± 3.79	61.74 ± 6.73	59.43 ± 3.79	63.65 ± 4.57	58.97 ± 5.5
	16	57.01 ± 4.44	65.08 ± 2.14	62.21 ± 0.72	66.05 ± 1.57	63.63 ± 4.74
Emotion (13)	4	09.18 ± 3.14	11.71 ± 2.16	11.65 ± 3.21	11.94 ± 1.95	11.03 ± 2.98
	8	11.18 ± 2.95	12.90 ± 1.63	10.56 ± 2.85	13.42 ± 1.46	12.38 ± 2.69
	16	12.32 ± 3.73	13.38 ± 2.20	11.62 ± 3.11	14.03 ± 2.35	12.32 ± 1.76
Sentiment Books (2)	4	73.15 ± 5.85	82.54 ± 1.33	76.95 ± 1.03	83.22 ± 0.95	74.51 ± 5.25
	8	75.46 ± 6.87	83.03 ± 1.28	77.49 ± 1.08	83.8 ± 0.8	79.25 ± 1.97
	16	77.26 ± 3.27	83.33 ± 0.79	77.88 ± 0.56	83.8 ± 1.59	78.41 ± 1.08
Rating DVD (3)	4	47.73 ± 6.20	49.76 ± 9.80	45.91 ± 9.85	45.2 ± 8.91	39.64 ± 5.17
	8	47.11 ± 4.00	53.28 ± 4.66	47.23 ± 9.22	58.38 ± 2.9	52.35 ± 5.27
	16	48.39 ± 3.74	53.52 ± 4.77	48.49 ± 8.88	57.41 ± 4.71	60.4 ± 3.71
Rating Electronics (3)	4	37.40 ± 3.72	51.71 ± 7.20	44.47 ± 8.25	45.34 ± 7.22	39.53 ± 5.76
	8	43.64 ± 7.31	54.78 ± 6.48	49.1 ± 6.81	55.10 ± 5.12	47.83 ± 5.94
	16	44.83 ± 5.96	58.69 ± 2.41	50.68 ± 6.8	59.47 ± 2.29	56.53 ± 4.36
Rating Kitchen (3)	4	44.72 ± 9.13	50.21 ± 09.63	45.38 ± 10.96	45.20 ± 8.78	39.11 ± 7.16
	8	46.03 ± 8.57	53.72 ± 10.31	46.71 ± 9.84	54.53 ± 9.9	50.19 ± 8.36
	16	49.85 ± 9.31	57.00 ± 08.69	52.87 ± 9.52	58.94 ± 7.58	57.63 ± 8.37
Political Audience (2)	4	51.47 ± 3.68	52.60 ± 3.51	52.45 ± 4.26	54.1 ± 3.66	52.03 ± 2.73
	8	51.83 ± 3.77	54.31 ± 3.95	52.87 ± 4.31	56.01 ± 3.65	52.06 ± 2.27
	16	53.53 ± 3.25	57.71 ± 3.52	55.6 ± 1.85	58.57 ± 2.04	54.33 ± 3.14
Sentiment Kitchen (2)	4	62.71 ± 9.53	78.35 ± 18.36	69.81 ± 14.58	81.96 ± 3.73	72.73 ± 7.97
	8	70.19 ± 6.42	84.88 ± 1.12	75.76 ± 1.13	83.33 ± 1.99	76.86 ± 4.46
	16	71.83 ± 5.94	85.27 ± 1.31	76.41 ± 0.66	84.33 ± 1.81	80.78 ± 4.38
Disaster (2)	4	50.87 ± 1.12	51.45 ± 4.25	49.76 ± 4.73	55.03 ± 8.73	52.62 ± 2.71
	8	51.30 ± 2.30	55.96 ± 3.58	52.17 ± 5.17	57.77 ± 6.40	55.04 ± 5.79
	16	52.76 ± 2.92	61.32 ± 2.83	55.37 ± 4.53	65.18 ± 4.41	62.27 ± 4.42
Airline (3)	4	40.27 ± 8.19	54.95 ± 11.81	57.11 ± 14.16	57.39 ± 7.83	51.62 ± 10.53
	8	51.16 ± 7.60	61.44 ± 03.90	64.37 ± 3.49	65.67 ± 4.82	57.47 ± 9.37
	16	48.73 ± 6.79	62.15 ± 05.56	66.31 ± 2.55	69.48 ± 2.06	65.02 ± 5.16
Rating Books (3)	4	48.44 ± 7.43	54.92 ± 6.18	56.57 ± 8.17	55.79 ± 5.61	54.4 ± 5.83
	8	52.13 ± 4.79	59.16 ± 4.13	57.33 ± 7.63	65.74 ± 5.58	57.17 ± 6.77
	16	57.28 ± 4.57	61.02 ± 4.19	63.26 ± 3.59	67.87 ± 3.45	66.66 ± 3.93
Political Message (9)	4	14.22 ± 1.25	15.69 ± 1.57	14.58 ± 1.78	18.84 ± 1.82	14.96 ± 1.94
	8	15.67 ± 1.96	18.02 ± 2.32	15.13 ± 2.16	20.09 ± 2.71	16.09 ± 2.6
	16	16.49 ± 1.96	18.07 ± 2.41	16.38 ± 2.15	23.22 ± 1.17	16.62 ± 2.19
Sentiment DVD (2)	4	74.38 ± 2.44	80.32 ± 1.02	72.03 ± 11.61	80.97 ± 1.21	73.08 ± 7.56
	8	75.19 ± 2.56	80.85 ± 1.23	75.79 ± 1.62	81.85 ± 1.79	76.55 ± 2.9
	16	75.26 ± 1.07	81.25 ± 1.41	76.69 ± 0.8	83.48 ± 1.01	78.19 ± 1.32
Scitail (2)	4	76.27 ± 4.26	69.50 ± 9.56	59.13 ± 10.58	53.48 ± 5.59	61.55 ± 9.11
	8	78.27 ± 0.98	75.00 ± 2.42	62.63 ± 10.85	60.79 ± 4.6	68.03 ± 4.54
	16	78.59 ± 0.48	77.03 ± 1.82	68.03 ± 1.57	61.67 ± 3.61	68.5 ± 3.7
Restaurant (8)	4	17.36 ± 2.75	49.84 ± 3.31	13.37 ± 2.25	27.00 ± 2.61	20.31 ± 2.97
	8	18.70 ± 2.38	62.99 ± 3.28	16.83 ± 3.42	35.66 ± 2.39	27.74 ± 2.29
	16	16.41 ± 1.87	70.44 ± 2.89	16.0 ± 3.44	37.20 ± 2.68	28.57 ± 2.41
CoNLL (4)	4	32.23 ± 5.10	54.16 ± 6.32	31.31 ± 5.32	40.79 ± 3.40	36.07 ± 3.25
	8	34.49 ± 5.15	67.38 ± 4.33	33.17 ± 5.1	41.25 ± 5.21	40.5 ± 2.16
	16	33.75 ± 6.05	76.37 ± 3.08	34.04 ± 3.59	45.96 ± 4.75	43.67 ± 6.92

Table 6: Classification performance (accuracy) of MetaSLP and baselines in the high-resource setting. Entries in green indicate the best model out of all; * refers to the baseline as reported in Bansal et al. (2020a). Each set of results is separated by a double line. The first set of results contains intent classification tasks, the second set has a natural language inference task and the last set contains entity typing tasks.

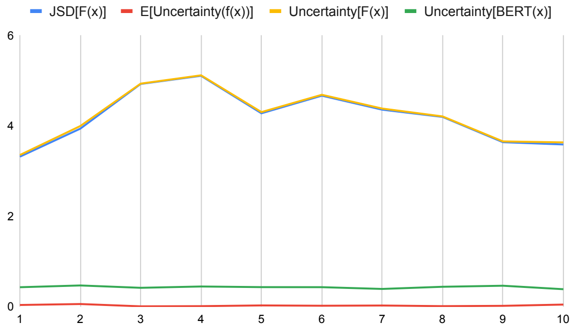

Figure 9: Ensemble uncertainty contrasted against the uncertainty of fine-tuned BERT, where we observe that DeepSLP's uncertainty $F(x)$ (given by yellow) is driven by ensemble diversity, given by $JSD(F(x))$ in blue.

individual models and the ensemble. We use this definition to ascertain the diversity of classifications provided by the jointly utilised soft-label prototypes. Diversity is a desirable property as ensemble predictions are generally more robust due to diversity between the predictions of their individual members (Lee et al., 2015).

Existing work (Ashukha et al., 2020; Lakshminarayanan et al., 2017) defines ensemble uncertainty as the sum of ensemble diversity and the expected average model uncertainty on ood data. Based on Abe et al. (2022), it is calculated as:

$$H([y|F(x)] = \frac{-1}{C}\sum p(y_i|F(x))log(p(y_i|F(x)))$$

If we use the Jenson-Shannon divergence as a diversity measure for an ensemble given by

$$JSD_{p(f)}[y|f(x)] = \frac{1}{M}\sum KL[y|f(x)||y|F(x)]$$

where KL is the average KL divergence between the output distribution of each soft-label prototype and the jointly utilised soft-label prototypes, from Abe et al. (2022), this expression reduces to:

$$H([y|F(x)] = \overbrace{JSD_{p(f)}[y|f(x)]}^{ens.\ diversity} + \overbrace{E_{p(f)}[H[y|f(x)]]}^{avg.\ model\ uncert.}$$

We contrast ensemble uncertainty and single model uncertainty using the fine-tuned BERT model for the task *airline* in Figure 9, but note that similar trends are observed across all tasks. We note that the uncertainty of jointly utilised soft-label prototypes is generally higher than that of the fine-tuned BERT model. As the average model uncertainty of individual soft-label prototypes is negligibly low, the uncertainty in the joint case is driven mainly by the diversity of the ensemble. This is in line with previous work which attributes an increase in uncertainty in ensembles due to diversity (Lakshminarayanan et al., 2017; Dietterich, 2000; Wilson and Izmailov, 2020). Though not strictly an ensemble, our approach exhibits similar properties (higher uncertainty driven by model diversity), as well as a general reduction in standard deviation compared to fine-tuned BERT.

The above provide evidence that our approach as a whole exhibits desirable properties of ensembles which drive a higher performance but which do not lead to higher training time nor compute.